

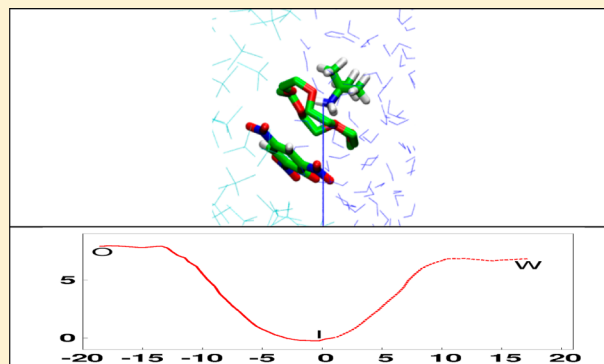
Ammonium Recognition by 18-Crown-6 in Different Solutions and at an Aqueous Interface: A Simulation Study

G. Benay and G. Wipff*

Laboratoire MSM, UMR 7177, Institut de Chimie, 1 rue B. Pascal, 67000 Strasbourg, France

 Supporting Information

ABSTRACT: The complexation of alkylammonium RNH_3^+ cations by 18-crown-6 (18C6) is studied by molecular dynamics (MD) and potential of mean force (PMF) simulations in different solvents (methanol, chloroform, 90:10 chloroform/methanol mixture, water) and at the chloroform/water interface. The free energies of association ΔG_{ass} , obtained with different charge models of 18C6, are compared for PrNH_3^+ and K^+ cations yielding, with suitable electrostatic models, a preference for K^+ in the different monophasic solutions, as well as in the gas phase. Furthermore, for a given cation, ΔG_{ass} is markedly solvent dependent and decreases in magnitude in the order chloroform \gg mixture > methanol > water, that is, with the (de)solvation energy of the cation and with the extent of pairing with the counterion (here, picrate, Pic^-). Despite their macroscopic immiscibilities at all proportions, chloroform and methanol are found to form, at the microscopic level, an inhomogeneous liquid that displays dual solvation properties toward its solutes. As a result, in the monophasic 90:10 mixture that contains mainly chloroform, the ΔG_{ass} energies for PrNH_3^+ or K^+ complexation are closer to those in methanol than to those in chloroform. On the other hand, chloroform and water form a biphasic mixture and delineate an interface onto which 18C6 and the $t\text{BuNH}_3^+$ and Pic^- ions, as well as their complex, are found to adsorb, a feature also supported by the different free energy profiles for interface crossing. Interestingly, the complexation energy of $t\text{BuNH}_3^+$ is found to be stronger at the interface than in pure water, demonstrating the crucial role of complexation by 18C6 at the interface to promote the cation transfer to the organic phase.



INTRODUCTION

The complexation and recognition of primary organic or biogenic ammonium cations by specific receptors represents a beautiful case of molecular recognition in supramolecular chemistry and biology. Important insights into the energy and stereochemistry of the related interactions have been gained from studies with synthetic macrocyclic hosts like cryptands, calixarenes, cyclopeptides, crown ethers (for a recent review, see for instance ref 1). Among these, the 18-crown-6 macrocycle (18C6) and its derivatives or aza analogues have been recognized early as strong binders of RNH_3^+ cations in solution.^{2–12} Complexation typically involves “linear” H-bonds between RNH_3^+ protons and the O (or N) binding sites of the crown ether that tends to adopt a pseudo- D_{3d} symmetry,^{13–15} as in the 18C6/ H_3O^+ complex.^{16,17} In the gas phase, the enthalpy of complexation ΔH_c with 18C6 is quite high (-46 kcal/mol for the 18C6/cyclohexylammonium complex),¹⁸ whereas in solution, it is much smaller (-1.5 kcal/mol in water and -12.0 kcal/mol in methanol for the benzylammonium cation¹⁵), as generally observed with hydrophilic ions.¹⁹ Furthermore, in solution, strong contributions from entropy terms counteract the enthalpy.^{15,20,21} The solvent is often chosen for practical reasons, such as the solubility of the salt, the host, and their complex, or characterization methods in a

given series. For instance, Izatt et al. studied by calorimetry complexes of 18C6 with 30 organic ammonium cations in methanol,²² while Lehn et al. used a chloroform/methanol mixture (90:10 ratio) to follow by NMR the recognition of linear diammonium cations by ditopic receptors incorporating crown ether binding sites.¹¹ Chloroform/methanol mixtures have also been used to conduct thermodynamics studies on cation–macrocyclic interactions.^{23–30} Cram et al. used another characterization method, based on the extraction of a salt (for instance $t\text{BuNH}_3^+ \text{ SCN}^-$) from an aqueous to a chloroform phase by the crown-ether.^{2–4,31} An indirect estimation of the free energy of association of $t\text{BuNH}_3^+$ with 18C6 “in chloroform” was $\Delta G_c = -8.8$ kcal/mol.³¹

Besides thermodynamic parameters, it is essential to understand at the microscopic level the interplay between solvation forces, the state of ion pairs and host/guest interactions, and to obtain a detailed description of the solvent effect on the complexation mechanism. For that purpose, molecular dynamics MD simulations and related free energy calculations are quite useful, as is the well studied case of alkali

Received: August 19, 2014

Revised: October 21, 2014

Published: November 6, 2014



Table 1. Characteristics of the Simulated Solutions^a

number of solute molecules	solvent	box size (Å ³)	C _i (M)	simulation time (ns)
PrNH ₃ ⁺ Pic ⁻	180 CHCl ₃ + 25 MeOH	30 × 30 × 30		2 ^b + 3
	1476 CHCl ₃ + 205 MeOH	60 × 60 × 60		2 ^b + 3
PrNH ₃ ⁺ Pic ⁻	1600 CHCl ₃	60 × 60 × 60	0.008	2 + 16 (PMF)
PrNH ₃ ⁺ Pic ⁻	1476 CHCl ₃ + 205 MeOH	60 × 60 × 60	0.008	2 + 16 (PMF)
PrNH ₃ ⁺ Pic ⁻	3244 MeOH	60 × 60 × 60	0.008	2 + 16 (PMF)
PrNH ₃ ⁺ 18C6 Pic ⁻	1598 CHCl ₃	60 × 60 × 60	0.008	2 + 60 (PMF)
PrNH ₃ ⁺ 18C6 Pic ⁻	1476 CHCl ₃ + 205 MeOH	60 × 60 × 60	0.008	2 + 60 (PMF)
PrNH ₃ ⁺ 18C6 Pic ⁻	3226 MeOH	60 × 60 × 60	0.008	2 + 16 to 160 (PMF)
PrNH ₃ ⁺ 18C6 Pic ⁻	7070 H ₂ O	60 × 60 × 60	0.008	2 + 60 (PMF)
tBuNH ₃ ⁺ 18C6 Pic ⁻	7073 H ₂ O	60 × 60 × 60	0.008	2 + 60 (PMF)
K ⁺ 18C6 Cl ⁻	869 H ₂ O	30 × 30 × 30	0.061	2 + 1 to 52 (PMF)
K ⁺ 18C6 Cl ⁻	388 MeOH	30 × 30 × 30	0.061	2 + 14 to 52 (PMF)
K ⁺ 18C6 Pic ⁻	186 CHCl ₃	30 × 30 × 30	0.061	2 + 20 to 75 (PMF)
K ⁺ 18C6 Pic ⁻	180 CHCl ₃ + 25 MeOH	30 × 30 × 30	0.061	2 + 20 to 75 (PMF)
tBuNH ₃ ⁺ 18C6 Pic ⁻	801 CHCl ₃ /3540 H ₂ O	60 × 60 × (30 + 30)	0.016 ^c	2 + 60 (PMF)
tBuNH ₃ ⁺ Pic ⁻	476 CHCl ₃ /2084 H ₂ O	40 × 40 × (40 + 40)	0.026 ^c	2 + 60 (PMF)
18C6	468 CHCl ₃ /2121 H ₂ O	40 × 40 × (40 + 40)	0.026 ^c	2 + 60 (PMF)
tBuNH ₃ ⁺ 18C6 Pic ⁻	471 CHCl ₃ /2088 H ₂ O	40 × 40 × (40 + 40)	0.026 ^c	2 + 60 (PMF)
18C6/tBuNH ₃ ⁺ , 29 tBuNH ₃ ⁺ , 29 18C6, 30 Pic ⁻	272 CHCl ₃ /1598 H ₂ O	40 × 40 × (40 + 40)	0.777 ^c	5

^aSimulations at 300 K, unless otherwise indicated. ^bSimulation at 350 K to mix the liquids. ^cConcentration in water.

cations complexation by 18C6.^{32–37} On the computational side, because of the many structural and thermodynamic data available for macrocyclic complexes, the latter represent an excellent field to test and develop simulation methodologies also used in less well documented and more complex systems, as in biology. Regarding ammonium complexes of 18C6, they have been, to our knowledge, simulated by MD so far only in the gas phase.^{14,15}

In this paper, we report MD and potential of mean force (PMF) studies on the complexation of RNH₃⁺ cations by 18C6 in solutions inspired by these above-mentioned experiments, selecting Pic⁻ (picrate = trinitrophenolate) as the counterion. More specifically, we focus on mono- and biphasic solutions involving methanol, chloroform, water, and selected mixtures. First, the complexation of PrNH₃⁺ Pic⁻ by 18C6 is studied in the monophasic 90:10 chloroform/methanol mixture, as well as in the pure liquid components, in water and in the gas phase, for comparison. This allows us to compare the free energies of complexation in methanol and in water to experiments,²² and to benchmark the electrostatic representation of 18C6. The state of the uncomplexed PrNH₃⁺ Pic⁻ ion pair is also investigated in the three nonaqueous liquids. Furthermore, to get insights into the binding selectivity of 18C6 for the spherical K⁺ cation over the tetrahedral RNH₃⁺ ones, we calculate the corresponding complexation energies in the gas phase, in water, and in methanol solutions where experimental data are available,¹⁵ as well as in chloroform and its 90:10 mixture. The second simulated system is the biphasic chloroform/water mixture, where the complexation and extraction of tBuNH₃⁺ Pic⁻ by 18C6 are studied by PMF and MD simulations. We first compute the free energy of complexation at the interface and in pure water, as a reference. Then, to gain insights into the tBuNH₃⁺ Pic⁻ extraction by 18C6, we calculate the free energy profiles for transferring these species “alone”, as well as their complex, across the aqueous interface. This extends our previous work on liquid–liquid interfaces involved in ion extraction by macrocyclic hosts (such as 18C6,³⁸ 222 cryptand,³⁹ calixarenes⁴⁰) or classical amphiphilic extractants (such as TBP,⁴¹ amides,⁴² CMPO,⁴³

aza-ligands),^{44,45} as well as other MD and PMF studies on interface crossing by ions and their complexes.^{46–50}

METHODS

MD Simulations of Solutions. Molecular dynamics simulations were performed with the modified AMBER10 software⁵¹ with the following representation of the potential energy U:

$$U = \sum_{\text{bond}} k_l(l - l_0)^2 + \sum_{\text{angle}} k_\theta(\theta - \theta_0)^2 + \sum_{\text{dihedrals}} \sum_n V_n(1 + \cos(n\varphi - \gamma)) + \sum_{i < j} \left[\frac{q_i q_j}{R_{ij}} - 2\epsilon_{ij} \left(\frac{R_{ij}^*}{R_{ij}} \right)^6 + \epsilon_{ij} \left(\frac{R_{ij}^*}{R_{ij}} \right)^{12} \right] \quad (1)$$

It accounts for the deformation of bonds, angles, dihedral angles, and electrostatic and van der Waals interactions (assumed to be pairwise additive in this 1–6–12 potential), using the force field parameters of Cornell et al.⁵² The solvents were represented explicitly, using the united atom model for MeOH of Jorgensen,⁵³ the model for CHCl₃ of Chang et al.,⁵⁴ and TIP3P water⁵⁵ to study the RNH₃⁺ complexes. The 1–4 van der Waals and Coulombic interactions were divided by 2.0 and 1.2, respectively. The atomic charges of Pic⁻ and RNH₃⁺ ions were fitted on electrostatic potentials (ESP Merz–Kollman procedure implemented in Gaussian 09⁵⁶) using the 6-31G(d,p) basis set, at either HF or DFT levels (see Supporting Information, Table S1). For 18C6 (D_{3d} structure), the resulting ESP q_0 charges are either –0.305 e (DFT level) or –0.34 e (HF level). We decided however to use two other sets of charges. The first comes from refs 57 and 58 ($q_0 = -0.4$ e) where satisfactory PMF results on K⁺ complexation by 18C6 in water have been obtained, thus allowing us to consistently compare the K⁺ to RNH₃⁺ complexes. The second set, more polar, is obtained by scaling the previous charges by 1.5, yielding $q_0 = -0.6$ e, as used in early studies on alkali ions

complexation by 18C6 to mimic the polarization of 18C6 by the cation.³² An intermediate set with $q_O = -0.5$ e was also tested. The assessment of these sets regarding the complexation of RNH_3^+ ions with 18C6 in the gas phase as well as in aqueous and methanol solutions where experimental data are available, will be presented in the Results Section. Note that other studies used lower q_O charges (-0.34 e in the CHARMM force field) to simulate the K^+ complexation in water or methanol⁵⁹ or ammonium complexes in the gas phase.¹⁵ To test the effect of polarization on the complexation energies and on the interfacial behavior of 18C6 and its complex, we additionally performed “POL” simulations where polarization is described in AMBER via atomic polarizabilities for the solvents (POL3 water,⁶⁰ polarizable chloroform from ref 54, and methanol from ref 61), for 18C6 and the ions (see Supporting Information, Table S2). Nonbonded interactions were calculated with a 12 Å atom-based cutoff, correcting for the long-range electrostatics by using the Ewald summation method (PME approximation).⁶² The solutions were simulated with 3D-periodic boundary conditions. Their characteristics are given in Table 1.

All systems were first relaxed by 3000 steps of energy minimization and by a MD simulation of 0.5 ns at 300 K and a constant pressure of 1 atm to adjust the densities. Subsequent dynamics was performed at constant volume. The temperature was maintained at ca. 300 K by coupling the solution to a thermal bath using the Berendsen algorithm⁶³ with a relaxation time of 0.2 ps. The MD trajectories and velocities were calculated using the Verlet algorithm with a time step of 2 fs, in conjunction with SHAKE constraints on O–H, C–H, and N–H bonds.

Analysis of the Trajectories. The trajectories were saved and analyzed every picosecond using our MDS software and VMD⁶⁴ for pictures. Interaction energies between selected groups were calculated using the Ewald summation.

Potential of Mean Force (PMF) Calculations. To quantitatively assess the interactions between X and Y species in solution, we calculated the change in Helmholtz free energy $\Delta A(d)$ as a function of their separating distance. This was achieved using the thermodynamic integration method (TI) based on eq 2,

$$\begin{aligned}\Delta A &= \int_0^1 \left\langle \frac{\partial U}{\partial \lambda} \right\rangle_\lambda d\lambda \\ &\approx \sum_{i=1}^{1/\Delta\lambda} \frac{1}{2} \left(\left\langle \frac{\partial U}{\partial \lambda} \right\rangle_{i-1} + \left\langle \frac{\partial U}{\partial \lambda} \right\rangle_i \right) \Delta\lambda\end{aligned}\quad (2)$$

where the summation is approximated by a discrete summation over small steps (“windows”), and averaged over two consecutive steps using the trapezoidal approximation rule.⁶⁵ Here, the reaction coordinate is the CM(X)...CM(Y) distance d , where “CM” is the center-of-mass, and d is stepwise increased from d_0 (initial state $\lambda = 0$) to d_1 (final state $\lambda = 1$): $d = (1 - \lambda)d_0 + \lambda d_1$. We modified AMBER10 to fix d by an holonomic constraint at a given λ step. At each step, the average of the mean force and the resulting ΔA change are calculated. The dissociation PMFs of 18C6... RNH_3^+ and of RNH_3^+ ...Pic[−] generally started from the “complexed” state “C” ($\lambda = 0$) and ended with the dissociated state “D” ($\lambda = 1$) via intermediate steps, using increments of $\Delta d = 0.2$ Å; that is, $\Delta\lambda = 0.025$. To calculate the PMFs for interface crossing by a solute S ($S = 18\text{C}6$ or $t\text{BuNH}_3^+$ Pic[−] alone or their complex), the reaction coordinate was the CM(S)...CM(System) distance where

“System” denotes the whole simulated box, and we used Δd steps of 0.5 Å, as in a previous work.^{41,45} The resulting $\Delta A(d)$ curve was shifted to $\Delta A(z)$, where z is the distance between CM(S) and the “interface” (Gibbs dividing surface with $z = 0$, defined by the crossing between the water and chloroform density curves recalculated at every step). At each λ step, we performed 0.5 ns of equilibration plus 1.0 ns of data collection and averaging, requiring 75 ns to cover a separation distance of 10 Å along the dissociation PMF of the complex. These PMFs are noted $\text{PMF}_{0.5+1.0}$ in short. Tests with shorter or longer sampling ($\text{PMF}_{0.2+0.2}$ or $\text{PMF}_{0.5+3.5}$), as well as tests for hysteresis, have also been achieved, showing some decrease in the stability of the complexes when the sampling is increased. When compared to recent PMF simulations on protein–protein⁶⁶ or steroid–cyclodextrin associations,⁶⁷ these simulation times are shorter, but higher than those used in a previous $\text{PMF}_{0.0075+0.015}$ study on K^+ complexation by 18C6 in water.^{57,58} They allow, for instance, a sampling of different orientations of 18C6 and RNH_3^+ at a given d distance without using accelerating tools like replica exchange MD.⁶⁸ An illustration is given in Supporting Information, Figure S1, showing cumulated positions of 18C6 and PrNH_3^+ , their relative angle Θ , and the order factor $S(\Theta)$ that is close to zero on the average, at a given step.

Because of the imposed constraints and of the incomplete sampling, the PMF curves do not exactly correspond to the free energy of association ΔA_{ass} (or ΔG_{ass} , at constant pressure, assumed to be similar for condensed phases), however.^{59,69–71} Some estimate of ΔG_{ass} can be obtained by calculating the association constant:

$$K_{\text{ass}} = \int_0^\infty 4\pi r^2 \exp(-A(r)/(RT)) dr \quad (3)$$

and from there deduce the free energy of association $\Delta G_{\text{ass}} = -RT \log K_{\text{ass}}$ (see for instance refs 72 and 73 for the case of simple ions association). In practice, the summation was carried up to the d_{max} distance of the PMF. The ΔG_{ass} energy is generally smaller in magnitude than the free energy minimum ΔA_{min} along the PMF. For instance, the Dang and Kollman’s PMF study of K^+ ...18C6 association reported $\Delta A_{\text{min}} \approx -7$ kcal/mol, and $\Delta G_{\text{ass}} \approx -3.5$ to -2.0 kcal/mol, depending on the integration mode. Likewise, in the PMF study of amide...amide interaction, Jorgensen noted that the well-depth in the free-energy profiles may be several kcal/mol more negative than the free energy of binding.⁷⁴ Furthermore, eq 3 assumes an isotropic distribution of X and Y species, and this hypothesis may overestimate the stability of the complex, by about 1.5 kcal/mol in the case of 18C6/ K^+ .⁵⁷ Thus, ΔG_{ass} values estimated with this procedure should be considered with care, when compared to experimental free energies of complexation ΔG_c . However, trends calculated from one solvent to the other or from a cation to the other with a same protocol should be meaningful.

QM Calculations. All structures were optimized at the DFT/B3LYP or HF levels of theory using the Gaussian 09 software.⁵⁶ Complexation or interaction energies were calculated with the 6-31G(d,p) and 6-311++G(d,p) basis sets and corrected from basis set superposition errors “BSSE” and the thermal thermodynamic contributions, as implemented in Gaussian 09.

Table 2. Complexation of K^+ and RNH_3^{+a} by 18C6 in the Gas Phase: Complexation Energy E_c , Free Energy ΔG and Enthalpy, Deformation Energy E_{deform} (kcal/mol), Average N–O Distance in the Complex (in Å). HF and DFT/B3LYP Calculations at the 6-311++G(d,p) Level

cation	K^+		$PrNH_3^+$		$BzNH_3^+$		$cyHexNH_3^+$		$tBuNH_3^+$		$\Delta PrNH_3^+ / tBuNH_3^+$		$\Delta K^+ / PrNH_3^+$	
	HF	DFT	HF	DFT	HF	DFT	HF	DFT	HF	DFT	HF	DFT	HF	DFT
E_c	-70.2	-70.3	-54.0	-56.7	-50.7	-53.1	-45.8	-48.7	-45.8	-48.8	8.2	7.9	16.2	13.6
ΔG^b	-57.7	-59.4	-36.8	-40.3	-33.4	-34.7	-30.2	-31.6	-29.3	-29.9	7.5	10.4	20.9	19.1
ΔH^b	-69.9	-68.7	-51.7	-54.2	-49.0	-51.8	-44.3	-46.1	-43.4	-48.0	8.3	6.2	18.2	14.5
E_{deform}^c	4.5		4.8		5.4		6.2		7.5		2.7		0.3	
$\langle d(N-O) \rangle$	2.81		2.99		3.01		3.10		3.10					

^aR = propyl (Pr), benzyl (Bz), cyclohexyl (CyHex), *tert*obutyl (*t*Bu). ^bThermodynamics corrections achieved at the 6-31G(d,p) level. A test on the $PrNH_3^+$ complex with the 6-311++G(d,p) basis sets yields a difference of only 0.1 kcal/mol. ^cDeformation energy of 18C6: $E_{\text{deform}} = E(18C6)$ within the complex – $E(18C6)$ uncomplexed.

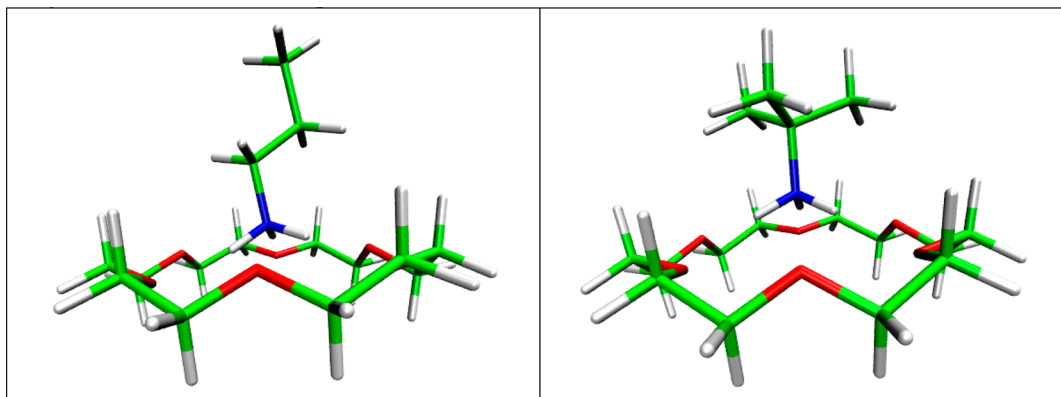


Figure 1. Snapshots of the optimized 18C6/ $PrNH_3^+$ (left) and 18C6/ $tBuNH_3^+$ complexes (right). DFT/6-311++G(d,p) calculations.

RESULTS

In the following, we first compare the complexation energy of selected RNH_3^+ cations (R = propyl, cyclohexyl, benzyl, *t*-butyl) and K^+ in the gas phase. We then analyze the state of the $PrNH_3^+$ Pic^- ion pair and the complexation of $PrNH_3^+$ and K^+ cations by 18C6 in different solvents and compare with experimental results in methanol and in water. Finally, the complexation and transfer of $tBuNH_3^+$ Pic^- by 18C6 at the chloroform/water interface are described.

(1). Interaction of 18C6 with alkyl NH_3^+ and K^+ Cations in the Gas Phase: QM and AMBER Results. Because gas phase and solution complexation experiments have been achieved with RNH_3^+ cations bearing different alkyl R groups, we first compare the complexation energy E_c of $PrNH_3^+$, $cyHexNH_3^+$, $BzNH_3^+$, and $tBuNH_3^+$ by 18C6 in the gas phase from QM minimized energies, with $E_c = E(\text{complex}) - E(\text{cation}) - E(18C6)$. This also allows us to benchmark the charge representation of 18C6 used in AMBER. Complexation enthalpies ΔH_c and free energies ΔG_c that include thermodynamic thermal contributions at 300 K have also been calculated. The HF and DFT results (see Table 2) show that both E_c and ΔG_c energies are strongest for the $PrNH_3^+$ complex and weakest for the $tBuNH_3^+$ one, thus decreasing in magnitude when the C(N) carbon gets more substituted. Snapshots of these complexes are shown in Figure 1. The difference $\Delta\Delta G_c$ between $tBuNH_3^+$ and $PrNH_3^+$ complexes amounts to 10.4 (DFT) or 7.5 (HF) kcal/mol. A similar trend has been observed in methanol solution and has been attributed to steric hindrance between the *t*Bu group of $tBuNH_3^+$ and 18C6.²² From an AMBER energy component analysis on the complex,

we find no evidence for such a repulsion (see Supporting Information, Table S3): both Coulombic and van der Waals interaction energy between 18C6 and the *t*Bu moiety are instead found to be attractive (-14.9 and -3.0 kcal/mol, respectively). QM calculations rather support the view that this relates to the higher charge dilution in the more polarizable *t*Bu group than in the Pr one: (for instance, $q_R = +0.56$ vs +0.46 e, respectively, with ESP charges; DFT results), thereby weakening the N–H···O bonds within the $tBuNH_3^+$ complex. As a result, the average N···O distances increase from 2.99 Å in the $PrNH_3^+$ complex to 3.10 Å in the $tBuNH_3^+$ complex. Both distances are comparable to those observed in X-ray structures.¹³ We note the complexed $PrNH_3^+$ cation is more “nested”, while $tBuNH_3^+$ is rather “perched” over the ring (see Figure 1). The deformation energy ΔE_{deform} of the host upon cation binding also contributes to the selectivity: according to HF calculations, ΔE_{deform} is 2.7 kcal/mol weaker in the $PrNH_3^+$ than in the $tBuNH_3^+$ complex (see Table 2).

Experimentally, an enthalpy of complexation of -46 kcal/mol has been reported for the $cyHexNH_3^+$ cation,¹⁸ which compares to our calculated values ΔH_c of -44.3 (HF level) or -46.1 kcal/mol (DFT level). The excellent fit observed at the DFT level suggests that the latter yields satisfactory predictions for the other cations. In the studied ammonium series, the sequence of E_c and ΔG_c (DFT or HF) energies is $PrNH_3^+ > BzNH_3^+ > cyHexNH_3^+ \geq tBuNH_3^+$. For the enthalpic component ΔH_c , the sequence is the same, excepted for $cyHexNH_3^+$ ($tBuNH_3^+ > cyHexNH_3^+$) at the DFT level.

The AMBER results depend, for a given cation model, on the choice of atomic charges on 18C6 (see Supporting Information, Table S4). Tests with $PrNH_3^+$ and q_O charges of -0.4, -0.5,

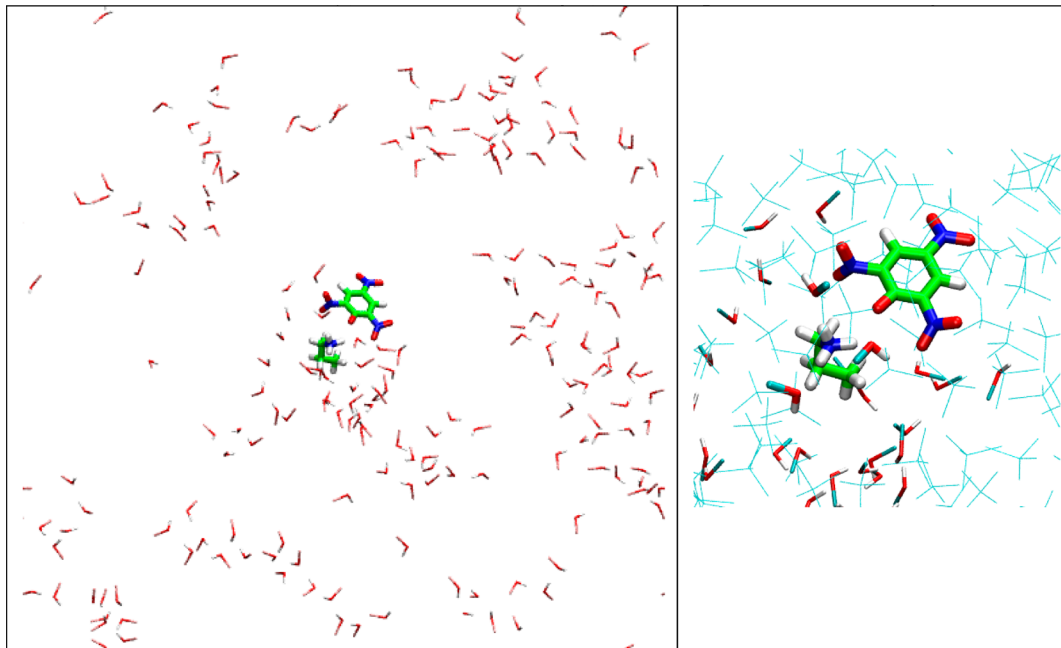


Figure 2. Snapshot of PrNH_3^+ Pic^- in the chloroform/methanol mixture: solvent box (left, chloroform hidden for clarity) and the solute (right). For the pure solvents see Supporting Information, Figure S3.

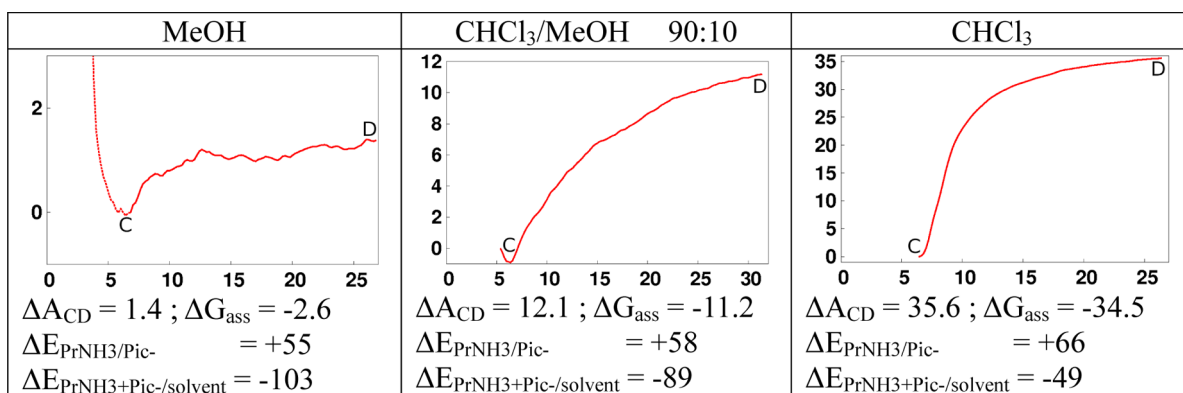


Figure 3. Dissociation PMF_{0.2+0.2} of the PrNH_3^+ Pic^- salt in three solvents: free energies ΔA (kcal/mol) as a function of the $\text{CM}(\text{PrNH}_3^+)$... $\text{CM}(\text{Pic})$ distance (in Å). ΔE energies correspond to the differences from C (complexed) and D (decomplexed) states. Snapshots at different positions are given in Supporting Information, Figure S4.

and -0.6 e on 18C6, yields E_c energies of -51.6 , -61.8 , and -71.4 kcal/mol, respectively. Since the results obtained with -0.4 and -0.6 charges bracket the DFT value (-56.7 kcal/mol), these two sets will be used to simulate the complexation reaction in solution. Comparing now the PrNH_3^+ to $t\text{BuNH}_3^+$ complexes (see Supporting Information, Table S5), one sees that AMBER accounts for the higher stability of the former (by $\Delta E_c = 1.3$ or 3.3 kcal/mol with $q_0 = -0.4$ or -0.6 e, respectively), but markedly underestimates the difference, presumably due to the lack of explicit account of polarization and electron transfer energy components in the force field.

Experimentally, the stability constants K of BzNH_3^+ and K^+ complexes with 18C6 has been consistently determined in different solvents (water, methanol, isopropyl alcohol, DMSO, DMF), revealing that the K^+ complex is the most stable, with a nearly linear correlation between the log K values of the two cations.¹⁵ In the gas phase, K^+ also forms a stronger complex than PrNH_3^+ , according to our QM and AMBER results (see E_c , ΔH_c , and ΔG_c energies in Table 2). The ΔE_c difference

between the two cations is again larger with HF or DFT methods (16.2 and 13.6 kcal/mol, respectively) than with AMBER (2.1 kcal/mol when $q_0 = -0.4$ e; 1.0 kcal/mol when $q_0 = -0.6$ e), also presumably due to the neglect of electron reorganization upon complexation in the AMBER force field. Comparing now for the K^+ complex the AMBER E_c energies to the reference DFT one (-70.3 kcal/mol), one observes the best agreement with q_0 charges of -0.6 e ($E_c = -72.4$ kcal/mol), while with charges of -0.4 or -0.5 e, E_c is underestimated ($E_c = -49.5$ and -61.1 kcal/mol, respectively; see Supporting Information, Table S4).

(2). Ion Pairing and Solvation of Uncomplexed Propylammonium Picrate in the 90:10 Chloroform/Methanol Mixture and in the Pure Solvents. Before examining the ammonium complexation process, we first investigated by MD and PMF simulations the state of the PrNH_3^+ Pic^- salt in methanol, in chloroform, and in the 90:10 mixture. MD simulations started with remote ions and were run for 2 ns. The evolution of d_+ distance $\text{CM}(\text{PrNH}_3^+)$... CM

(Pic^-) along the dynamics is shown in Supporting Information, Figure S2. In the mixture, the ions are most often in contact (see Figure 2), and d_+ oscillates between 4.2 and 10.3 Å. The salt (especially the NH_3^+ head) is surrounded by MeOH molecules, in its first shell and beyond. The nitro oxygens of Pic^- are less prone to form H-bonds with MeOH protons. Repeating the simulation in the pure solvents yields different outcomes (see Figure S2). In chloroform, pairing is stronger, as expected, and d_+ remains nearly constant, at ca. 6.1 Å. In methanol (and a fortiori in water), the ions are dissociated, at $d_+ \approx 25 \pm 6$ Å, oscillating from ca. 12 to 40 Å.

The above observations are consistent with free energy profiles for the $\text{PrNH}_3^+ \dots \text{Pic}^-$ dissociation (PMF_{0.2+0.2} procedure) in the three solutions (Figure 3). All curves display a minimum for the contact ion pair, at a separation distance of about 5 Å between CM(Pic^-) and the N(ammonium) atom, involving H-bonds between PrNH_3^+ protons and the O-phenolate and the adjacent NO_2 oxygens. From there, dissociating the ion pair to a distance of 25 Å costs 35.6 kcal/mol in chloroform, 12.1 kcal/mol in the mixture, and only 1.4 kcal/mol in methanol. The corresponding free energies of association ΔG_{ass} , calculated from eq 3 are -34.5 , -11.2 , and -2.6 kcal/mol, respectively. Since $\Delta A(d)$ curves have not reached a plateau at 25 Å, these numbers are likely underestimated, especially for the chloroform containing solutions. Note that in the 90:10 mixture where chloroform is in excess, the free energy of ion pairing is closer to the one in methanol than to the one in chloroform. The importance of solvation by methanol in the mixture is also highlighted by an energy component analysis along the dissociation PMFs (Supporting Information, Table S6): PrNH_3^+ and Pic^- get better solvated by a similar amount in methanol and in the mixture ($\Delta \approx -45$ and -56 kcal/mol, respectively for Pic^- , -56 and -54 kcal/mol for PrNH_3^+), which is about twice more than in pure chloroform.

(3). Complexation of $\text{PrNH}_3^+ \text{ Pic}^-$ by 18C6 in Chloroform, Methanol, Their 90:10 Mixture and in Water. Comparison with K^+ Complexation. To compare the stability of the 18C6/ $\text{PrNH}_3^+ \text{ Pic}^-$ complex in the four solvent environments, we calculated its dissociation PMF, that is, after 2 ns of equilibration, as a function of the d distance between CM(18C6) and CM(PrNH_3^+) that was gradually increased from ≈ 2 Å in the complexed state C to ca. 10 Å for the decomplexed D state, with either -0.4 , -0.5 , or -0.6 q_0 charges in water and in methanol solutions. Unless otherwise specified, the sampling was $0.5 + 1.0$ ns per step (PMF_{0.5+1.0}). The free energy curves and their ΔA_{CD} characteristics, grouped by solvents, are given in Figure 4, while those grouped by charges are given in Supporting Information, Figure S8. Table 3 gives a summary of calculated ΔG_{ass} energies and related experimental ΔG_c data in water and in methanol.

PrNH_3^+ in Methanol Solution. In the methanol solution, experimental complexation data have been reported for the 18C6/ MeNH_3^+ complex analogue ($\Delta G_c = -5.4$, $\Delta H_c = -11.7$ kcal/mol), indicating a high stability.¹⁵ We observed that when simulated with -0.4 q_0 charges, the complex dissociates after 1 ns (see Supporting Information, Figure S5), while the PMF_{0.5+1.0} affords an estimate of only -1.1 kcal/mol for ΔG_{ass} . Repeating the simulation with shorter or longer sampling (PMF_{0.2+0.2} or PMF_{0.5+3.5}) yields similar results ($\Delta G_{\text{ass}} = -1.2$ and -0.8 kcal/mol, respectively; see Figure S7), confirming that the stability of the complex is underestimated. In fact, when simulated with q_0 charges of -0.5 or -0.6 e, the complex

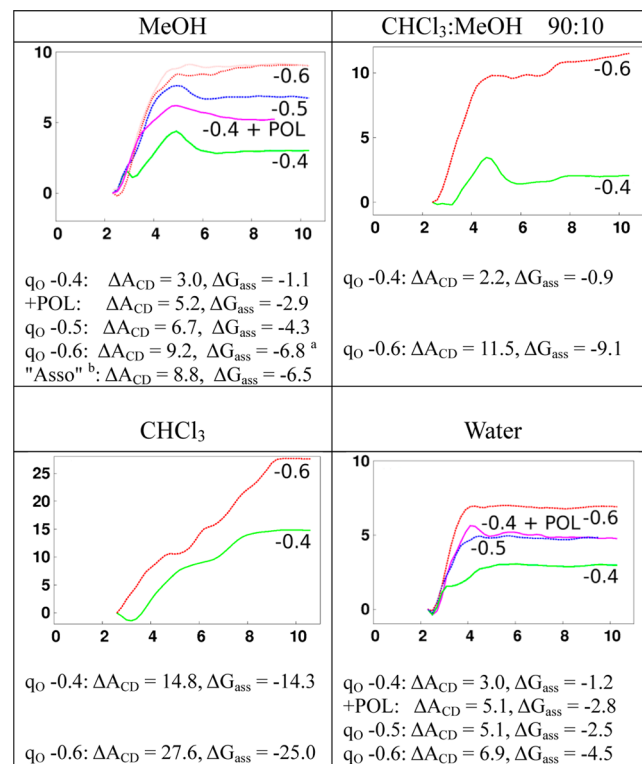


Figure 4. Complexation of $\text{PrNH}_3^+ \text{ Pic}^-$ by 18C6 in the four solvents. PMF_{0.5+1.0} calculated with different q_0 charges on 18C6 (-0.4 to -0.6 e): ΔA (in kcal/mol) as a function of the CM(PrNH_3^+)–CM(18C6) distance (Å). Energy components analysis along the PMF are shown in Supporting Information, Figure S6. For a comparison of different solvents simulated with a same 18C6 model see Figure S8. ^aIdentical energies are obtained when the PMF is pursued from 10 to 15 Å; ^bPMF of association (starting with the cation uncomplexed) instead of dissociation.

remains associated along 2 ns of dynamics, while the PMF_{0.5+1.0} results ($\Delta G_{\text{ass}} = -4.3$ or -6.8 kcal/mol, respectively) bracket the experimental value. To check for possible hysteresis issues we simulated the PMF for complex formation instead of dissociation, using the -0.6 q_0 charges, and starting at a d separation of 10 Å. The resulting ΔG_{ass} energy (-6.5 kcal/mol) is close to the one obtained from the dissociation pathway, indicating that there is no significant sampling issue in these PMF calculations.

PrNH_3^+ in Chloroform Solution. In chloroform, the 18C6/ PrNH_3^+ complex, simulated with either -0.4 or -0.6 q_0 charges on 18C6 turns out to be very stable, as seen from the PMF_{0.5+1.0} results: $\Delta G_{\text{ass}} = -14.3$ and -25.0 kcal/mol, respectively. When compared to the methanol solution, two main differences are noticed. The first one concerns the status of the Pic^- counterion that is always in contact with the PrNH_3^+ moiety, free or complexed in chloroform: when PrNH_3^+ is complexed, Pic^- sits on the same face of the crown and, as soon as the cation decomplexes, its freed protons form a tight ion pair with Pic^- . The second difference is the poorer solvation of PrNH_3^+ in chloroform, whether the cation be isolated or, a fortiori, paired with Pic^- (for instance, upon decomplexation, PrNH_3^+ gets better solvated, by only 9 kcal/mol in chloroform and by 50 kcal/mol in methanol, according to an energy component analysis).

PrNH_3^+ in the Chloroform/Methanol Mixture. We now turn to the PMF_{0.5+1.0} results in the 90:10 chloroform/methanol

Table 3. Calculated ΔG_{ass} Values (in kcal/mol) of 18C6/ M^+ / X^- Complexes from PMF_{t1+t2} Simulations with Different q_O Charge Sets on 18C6. Unless Otherwise Specified, the Simulations Are Performed without Polarization (NO-POL Model). The POL Results with Polarization Are Obtained with -0.4 Charges on 18C6. Comparison with Related ΔG_c Experimental Data

M^+ cation	X^-	$t1 + t2$ (ns)	q_O	ΔG_{ass}	ΔG_c exp
PrNH_3^+ in MeOH	Pic^-	0.5 + 1.0	-0.4	-1.1	-5.4 ^a
			-0.5	-4.3	
			-0.6	-6.8	
PrNH_3^+ in MeOH	Pic^-	0.2 + 0.2	POL	-2.9	-5.4 ^a
			-0.4	-14.3	
			-0.6	-25.0	
PrNH_3^+ in $\text{CHCl}_3:\text{MeOH}$	Pic^-	0.5 + 1.0	-0.4	-0.9	
			-0.6	-9.1	
			-0.8	-2.0 ^b	
PrNH_3^+ in TIP3P water	Pic^-	0.5 + 1.0	-0.4	-1.2	-2.0 ^b
			-0.5	-2.5	
			-0.6	-4.5	
PrNH_3^+ in POL3 water	Pic^-	0.2 + 0.2	POL	-2.8	-2.0 ^b
			-0.4	-1.9	-2.8
			-0.6	-4.7	
K^+ in TIP3P water	Cl^-	0.01 + 0.08	-0.4	-1.9	-2.8
			-0.6	-1.2	
			-0.8	-0.2	
			-1.0	-2.5	
			-1.2	-2.2	
			-1.4	-4.1	
			-1.6	-3.8	
			-1.8	-3.5	
			-2.0	-3.5	
K^+ in POL3 water	Cl^-	0.2 + 0.2	POL	-3.6	-2.8
K^+ in MeOH	Cl^-	0.2 + 0.2	-0.4	-1.1	-8.3
	Cl^-	0.5 + 1.0	-0.4	-0.2	
	Pic^-	0.2 + 0.2	-0.5	-5.3	
	Pic^-	0.5 + 1.0	-0.5	-6.6	
	Cl^-	0.5 + 1.0	-0.6	-7.4	
	Pic^-	0.5 + 1.0	-0.6	-7.8	
K^+ in MeOH	Cl^-	0.2 + 0.2	POL	-6.1	-8.3
K^+ in CHCl_3	Pic^-	0.2 + 0.2	-0.4	-28.4	
			-0.6	-36.3	
K^+ in $\text{CHCl}_3:\text{MeOH}$	Pic^-	0.5 + 1.0	-0.4	-3.7	
			-0.6	-12.8	
$t\text{BuNH}_3^+$ in TIP3P water	Pic^-	0.5 + 1.0	-0.6	-0.9	
$t\text{BuNH}_3^+$ at the $\text{CHCl}_3:\text{TIP3P}$ water interface	Pic^-	0.5 + 1.0	-0.6	-1.5	

^aObtained with MeNH_3^+ . See ref 15. ^bObtained with BzNH_3^+ . See ref 15.

mixture, obtained with either -0.4 or -0.6 q_O charges on 18C6. The resulting ΔG_{ass} energies (-0.9 and -9.1 kcal/mol) are close to those obtained in pure methanol, indicating that the complex is much weaker than in chloroform. The stability constant is not available in the solvent mixture, but it should be higher than in methanol and thus correspond to a ΔG larger in magnitude than 5.5 kcal/mol.¹⁵ The ΔG_{ass} energy obtained with -0.4 q_O charges is thus unsatisfactory, while the value obtained with -0.6 charges accounts for the high stability of the complex, likely exaggerated, though.

PrNH_3^+ in Aqueous Solution. In TIP3P water, the PMF_{0.5+1.0} has been calculated with q_O charges of -0.4 , -0.5 , and -0.6 e, yielding ΔG_{ass} energies of -1.2 , -2.5 , and -4.5 kcal/mol, respectively, that increase in magnitude with the q_O charges. The extreme values bracket the experimental value of -2.0 kcal/mol reported for the BzNH_3^+ complex analogue.¹⁵ With the -0.5 and -0.6 charge sets, the complex with PrNH_3^+ is correctly predicted to be less stable in water than in methanol. The results obtained with -0.4 charges are unsatisfactory, since the complex is not stable enough and dissociates after 4 ns of dynamics. Furthermore, they predict a nearly identical stability in water ($\Delta G_{\text{ass}} = -1.2$ kcal/mol) as in methanol (-1.1 kcal/mol), while experimentally the complex is much less stable in water (by $\Delta \Delta G_c \approx 3.4$ kcal/mol).

Comparison of K^+ to PrNH_3^+ Complexes with 18C6 in Four Solvents: Water, Methanol, Chloroform, and the 90:10 Mixture. To compare the K^+ to the PrNH_3^+ complexation in water, we first repeated the Dang and Kollman's PMF simulation,^{57,58} using their K^+ parameters, water model (SPC/E), 18C6 model (-0.4 q_O charges), and sampling (PMF_{0.01+0.08} simulation). Our results ($\Delta A_{\text{CD}} = 6.5$, $\Delta G_{\text{ass}} = -1.9$ kcal/mol; see Supporting Information, Figure S9) are identical to theirs, and within 0.1 kcal/mol the same as those we obtain with a higher sampling (PMF_{0.2+0.2} simulation; see Figure S9). The ΔG_{ass} energy is somewhat lower in magnitude than the experimental ΔG_c value of -2.8 kcal/mol.²⁰ The simulations were thus also performed with the -0.5 and -0.6 q_O charges, yielding the best fit ($\Delta G_{\text{ass}} = -2.7$ kcal/mol) with the former charge set. Repeating the PMF simulations in TIP3P instead of SPC/E water also yields the best fit with -0.5 charges ($\Delta G_{\text{ass}} = -2.5$ kcal/mol; see Table 3). Note that, for a given q_O set of charges, the complex is somewhat less stable in TIP3P than in SPC/E water (by up to $\Delta \Delta G_{\text{ass}} \approx 0.6$ kcal/mol), in keeping with the higher hydration energy of this K^+ ion in TIP3P water.⁷⁵ Regarding the somewhat higher stability of K^+ over PrNH_3^+ complexes in water (by $\Delta \Delta G_c = 0.8$ kcal/mol for the BzNH_3^+ analogue of PrNH_3^+), it is not predicted by PMF_{0.5+1.0} simulations with q_O charges of either -0.4 e ($\Delta G_{\text{ass}} = -0.2$ and -1.2 kcal/mol, respectively), -0.5 e ($\Delta G_{\text{ass}} = -2.2$ and -2.5 kcal/mol, respectively), or -0.6 e ($\Delta G_{\text{ass}} = -3.5$ and -4.5 kcal/mol, respectively).

In methanol, the preference for K^+ over PrNH_3^+ (experimental complexation energies ΔG_c are -8.3 and -5.4 kcal/mol, respectively)^{20,22} is qualitatively accounted for by PMF_{0.5+1.0} simulations using q_O charges of either -0.5 e ($\Delta G_{\text{ass}} \approx -6.6$ and -4.3 kcal/mol, respectively) or -0.6 e ($\Delta G_{\text{ass}} \approx -7.4$ and -6.8 kcal/mol, respectively), but the calculated selectivity ($\Delta \Delta G_{\text{ass}} = 2.3$ or 0.6 kcal/mol) is lower than the experiment value (2.9 kcal/mol). When simulated with q_O charges of -0.4 e, however, the K^+ complex turns out to be unstable: it dissociates after 1.4 ns of dynamics, while the PMF_{0.5+1.0} yields a too weak ΔG_{ass} values (-0.2 kcal/mol), wrongly predicting that the K^+ complex is less stable than the PrNH_3^+ one in methanol. Thus, regarding the electrostatic representation of 18C6, we see that the set with q_O charges of -0.4 e that has been previously used in a PMF study on the K^+ complexation in water^{57,58} underestimates the stabilities of the K^+ and PrNH_3^+ complexes in the gas phase, in methanol, and in water, and yields inconsistent stabilities in these solvents. Note that the X^- counterion may also modulate the ΔG_{ass} energies in methanol. For instance, replacing Cl^- by Pic^- in methanol stabilizes the 18C6/ K^+ complex (q_O charges of -0.6) by 0.4 kcal/mol (Table 3), presumably because Cl^- is less dissociated

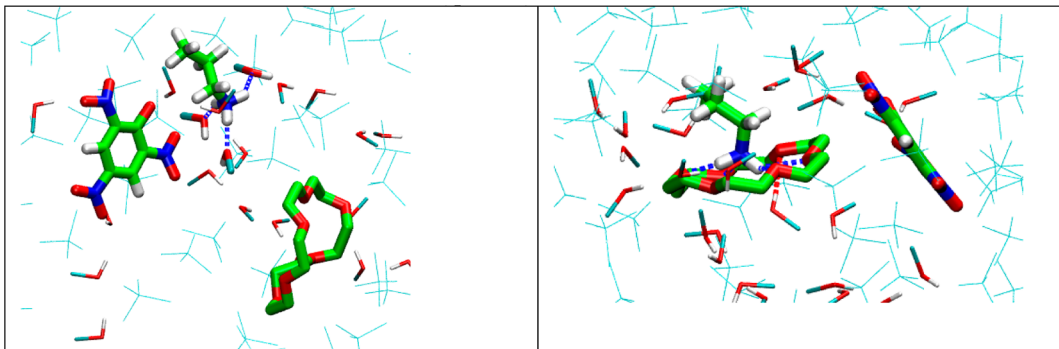


Figure 5. Snapshots of 18C6/PrNH₃⁺ Pic⁻ decomplexed (left) and complexed (right) in the 90:10 chloroform/methanol mixture ($q_O = -0.6$).

from the uncomplexed K⁺, requiring some energy penalty to complex K⁺.

Arguably, polarization effects can be important, and more important in methanol than in water. In the gas phase, methanol has a lower dipole moment than water ($\mu = 1.55$ and 1.83 D, respectively)⁷⁶ but it forms stronger complexes with cations like K⁺,⁷⁷ presumably because it has a higher polarizability than water ($\alpha = 3.3$ and 1.5 Å³, respectively).⁷⁶ Experimentally, the enthalpy of transfer of K⁺ from water to methanol is negative ($\Delta H_t = -4.5$ kcal/mol),⁷⁶ also hinting for stronger interactions of K⁺ with methanol. However, the free energy $\Delta G_t(K^+)$ is positive and unfavorable, because the entropic term is negative and dominant ($T\Delta S_t = -6.7$ kcal/mol).⁷⁶ Thus, the comparison of the complexation in the two solvents involves antagonistic enthalpy and entropy effects. These features led us to consistently calculate the PMF_{0.2+0.2} of K⁺ and PrNH₃⁺ dissociation in the two solvents using polarizable (POL) models and $-0.4 q_O$ charges on 18C6. The results are shown in Figure 4 for PrNH₃⁺ and in Figure 6 for K⁺ (purple $\Delta A(d)$ curves) and summarized in Table 3. From the NO-POL to the POL model, the stability of all complexes increases, by ~ 1.6 kcal/mol (PrNH₃⁺ in water) to 5.0 kcal/mol (K⁺ in methanol). In a given POL solvent, the K⁺ complex is now more stable than the PrNH₃⁺ one (by $\Delta\Delta G_{ass} = 0.8$ kcal/mol in water and 3.2 kcal/mol in methanol), in good agreement with the observed selectivities. Furthermore, K⁺ forms a stronger complex in methanol than in water (by $\Delta\Delta G_{ass} = 2.5$ kcal/mol), while for PrNH₃⁺ the difference (0.1 kcal/mol) is too weak. Thus, the experimental order of complexation free energies (PrNH₃⁺_{Water} < K⁺_{Water} < PrNH₃⁺_{Methanol} < K⁺_{Methanol}; $\Delta G_c = -2.0, -2.8, -5.4$, and -8.3 kcal/mol, respectively)¹⁵ is not fully reproduced with the POL model ($\Delta G_{ass} = -2.8, -3.6, -2.9$, and -6.1 kcal/mol, respectively), because the POL complexes are somewhat too stable in water (by 0.8 kcal/mol) and not enough stable in methanol (by 2.2 to 2.5 kcal/mol), likely due to inconsistencies between the two solvent models. What happens with other solvent and solute models remains to be investigated.

In pure chloroform and in its 90:10 mixture, no experimental data are available, but PMF_{0.5+1.0} simulations (NO-POL) carried out with $-0.6 e$ q_O charges on 18C6 yield ΔG_{ass} energies of -36.3 and -12.8 kcal/mol, respectively for K⁺ (see snapshots in Figure 5 and free energy curves in Figure 6). Thus, as for the PrNH₃⁺ cation, complexation in the mixture is more “methanol-like” ($\Delta G_{ass} = -7.4$ kcal/mol) than “chloroform-like”. Furthermore, K⁺ remains preferred over PrNH₃⁺ in chloroform and in the mixture, by 11.3 and 3.7 kcal/mol, respectively. Note that the difference (selectivity) in the

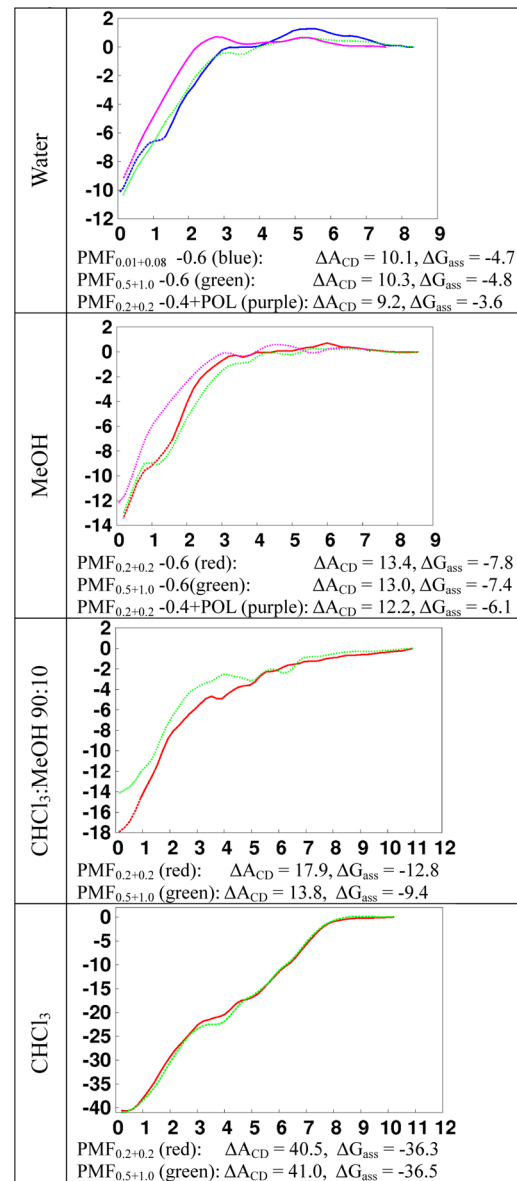


Figure 6. Complexation of K⁺ by 18C6 in different solvents ($q_O = -0.6$ e and $q_O = -0.4$ e + POL). Free energies (ΔA in kcal/mol) as a function of the K-CM(18C6) distance (Å), obtained with different sampling times. PMFs with other charges are shown in Supporting Information, Figure S9. Snapshots of the solvent box with dissociated and associated K⁺ complexes in the solvent mixture are shown in Figure S19.

mixture is again “methanol-like”. Similar features are found with the -0.4 charges on 18C6, but complexation energies are smaller, as expected.

(4). Complexation of $t\text{BuNH}_3^+$ Pic^- by 18C6 at the Chloroform/Water Interface and in Pure Water. The thermodynamics experiments of Cram et al. on RNH_3^+ complexation by crown ethers are based on a biphasic process, namely the distribution of $\text{RNH}_3^+ \text{X}^-$ salt (with for instance $\text{RNH}_3^+ = t\text{BuNH}_3^+$ and $\text{X}^- = \text{ClO}_4^-$, PF_6^- , SCN^- , or Pic^-) between deuterated water and chloroform, first in the absence, and then in the presence of the crown ether.^{2–4,31} From the measured guest to host ratio in the two phases, they afforded a consistent scale of stability constants. These studies motivated us to study what happens at the interface during this process, focusing on the $t\text{BuNH}_3^+$ Pic^- extraction. When compared to PrNH_3^+ , $t\text{BuNH}_3^+$ forms weaker complexes but is also more lipophilic and thus should behave somewhat differently at the interface.

The 18C6, $t\text{BuNH}_3^+$ Pic^- species were first simulated in a binary water/chloroform solution for 2 ns, starting where they are expected to be, that is, the salts in water, and 18C6 ($-0.6 q_0$ charges) in chloroform. However, along the dynamics, all three diffused to the interface, and remained there until the end (2 ns), indicating that they are surface active. Because this feature strongly supports a complexation mechanism occurring “right at the interface”, we decided to calculate the corresponding free energy profile (PMF_{0.5+1.0}), and to compare it with the one in pure water. In bulk water, the PMF simulation (see Figure 7)

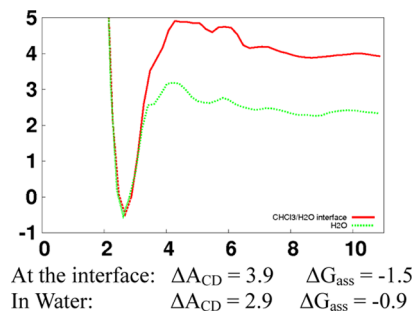


Figure 7. Complexation of $t\text{BuNH}_3^+$ by 18C6 ($q_0 = -0.6$) in water (green) and at the chloroform/water interface (red). PMF_{0.5+1.0}: free energies (ΔA in kcal/mol) as a function of the CM($t\text{BuNH}_3^+$)–CM(18C6) distance (Å). Snapshots of $t\text{BuNH}_3^+$ uncomplexed and complexed at the interface are given in Figure 8.

predicts that $t\text{BuNH}_3^+$ forms a weak complex ($\Delta G_{\text{ass}} = -0.9$ kcal/mol), weaker than the 18C6/ PrNH_3^+ one. This feature is supported by PMF results obtained with different charge models on the cations (see Supporting Information, Figure S10): using either DFT or HF charges yields $\Delta \Delta G_{\text{ass}} = 2.9$ or 3.0 kcal/mol, respectively. Note that the preference for PrNH_3^+ over $t\text{BuNH}_3^+$ is in good agreement with experimental complexation data with 18C6 in methanol ($\Delta \Delta G_c = 3.0$ kcal/mol)²² or extraction results with dicyclohexyl-18C6 ($\Delta \Delta G_c = 2.5$ kcal/mol “in chloroform”).⁷⁸

Repeating now the PMF calculation for $t\text{BuNH}_3^+$ complexation at the interface (see snapshots of the solvent box in Figure 8) yields $\Delta A_{\text{CD}} = 3.9$ kcal/mol and $\Delta G_{\text{ass}} = -1.5$ kcal/mol, indicating that the complex is somewhat more stable at the interface than in water ($\Delta A_{\text{CD}} = 2.9$ kcal/mol; $\Delta G_{\text{ass}} = -0.9$ kcal/mol). No experimental value is available with this cation neither in water nor, a fortiori, at the interface. We note that at the

interface, 18C6 and the cation are solvated by chloroform on one side and by water on the other side. However, as for the methanol/chloroform mixture, the energetics of solvation at the interface is mainly determined by the most polar solvent, here water (see an energy component analysis along the PMF in Supporting Information, Table S7). Thus, the complexation energy at the interface is more “water-like” than “chloroform-like”, but somewhat stronger than in pure water, though.

(5). Migration of $t\text{BuNH}_3^+$ Pic^- , 18C6, and of Their Complex Across the Chloroform/Water Interface. *Transfer of the $t\text{BuNH}_3^+$ Pic^- Salt.* The PMF for transferring the $t\text{BuNH}_3^+$ Pic^- salt has been calculated using three different reaction coordinates, defined by the distance d from the interface of the CM($t\text{BuNH}_3^+$ Pic^-), the CM($t\text{BuNH}_3^+$), or the CM(Pic^-), respectively. The solvent box is shown in Figure 9. The three $\Delta A(d)$ curves (Figure 10) confirm the preference of the ions for the aqueous over the organic phase, and the surface activity of the cation alone, the anion alone, or in combination. These curves however differ, due to different behaviors of the counterion. The main features are given below.

When the CM($t\text{BuNH}_3^+$ Pic^-) is pulled away from the interface, the two ions form a contact ion pair in chloroform and a loose or dissociated pair in water. The free energy difference ΔA_{IW} between the interface (I position) and bulk water (W position) amounts to 6.5 kcal/mol, while the ΔA_{IO} difference on the oil side (O position) is 14.4 kcal/mol. The difference ΔA_{OW} between the bulk phases is negative (-7.9 kcal/mol), supporting the lack of transfer of the salt alone.³¹ In principle, when only one ion is extracted to one phase, its counterion should follow it to keep every phase electroneutral. Along the PMF simulation, this turns out to be not always the case, though, since the counterion sometimes prefers to stay at the interface or in bulk water (see Figure 10). For instance, when $t\text{BuNH}_3^+$ is moved toward water, Pic^- remains at the interface, while when $t\text{BuNH}_3^+$ is moved toward the oil side, Pic^- follows it to form a tight ion pair. Likewise, when Pic^- is pulled to either bulk water or oil phases, $t\text{BuNH}_3^+$ oscillates from one interface to the other via the water phase without pairing with Pic^- . For the Pic^- transfer, the free energy minimum ΔA_{IW} with respect to the aqueous phase amounts to 5.5 kcal/mol, indicating that the anion alone, although lacking the amphiphilic topology, is more surface active than the $t\text{BuNH}_3^+$ cation ($\Delta A_{\text{IW}} = 2.1$ kcal/mol). Note that the sum of ΔA_{IW} energies for the ions “alone” (7.6 kcal/mol) is close to the ΔA_{IW} energy for the ion pair, in keeping with the fact that the ionic pair is dissociated in bulk water, as well as at the interface.

Transfer of the 18C6 Host Uncomplexed. The transfer of 18C6 uncomplexed across the interface has been first simulated with the two charge models, namely $q_0 = -0.4$ and -0.6 e, respectively. The free energy profiles are shown in Figure 11 and Supporting Information, Figure S12. With both models, a free energy minimum is observed “at the interface” (at $z \approx 0$ Å for the -0.6 model and more on the oil side, $z \approx -3$ Å, for the -0.4 model), demonstrating the surface activity of 18C6. At the interface, the crown oscillates between positions parallel and perpendicular to the xy plane, with one or two faces H-bonded to H_2O molecules, reminiscent of hydration patterns in water.⁷⁹ However, as reported for a small drug analogue,⁸⁰ its partitioning between the two phases, determined by the ΔA_{OW} difference, is found to be model dependent: with the $-0.6 q_0$ charges it prefers water ($\Delta A_{\text{OW}} \approx -5.0$ kcal/mol) while with the $-0.4 q_0$ charges it prefers chloroform ($\Delta A_{\text{OW}} \approx$

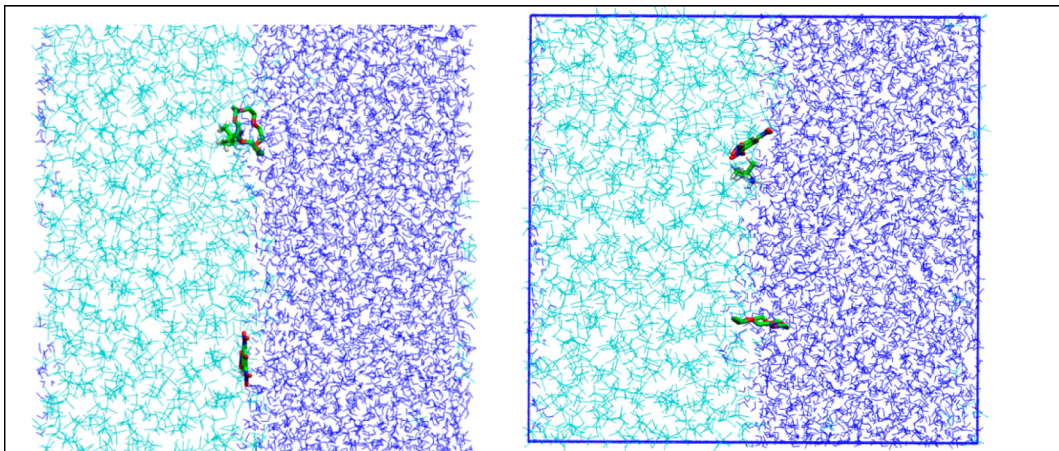


Figure 8. Complexation of $t\text{BuNH}_3^+$ by 18C6 at the chloroform/water interface: snapshots of $t\text{BuNH}_3^+$ complexed (left) and uncomplexed (right).

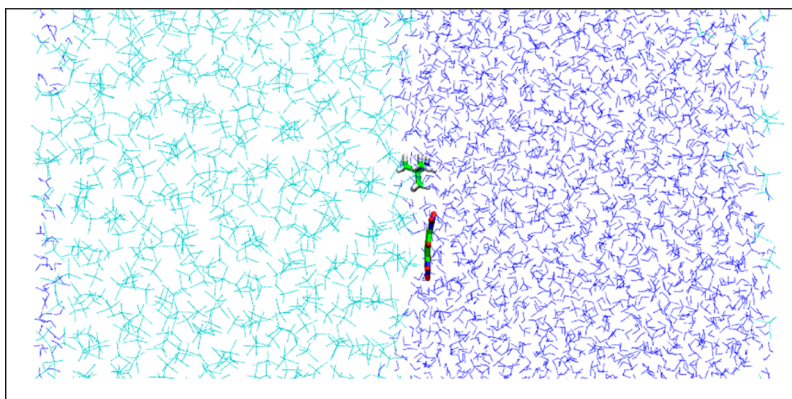


Figure 9. $t\text{BuNH}_3^+$ Pic^- at the chloroform/water interface: snapshot of the solvent box.

5.2 kcal/mol). Experimentally, 18C6 prefers chloroform, but about 15% is solubilized in water,³¹ indicating that the free energy difference between the two phases is weak. In fact, its extraction equilibria have been studied experimentally at different temperatures,⁸¹ yielding a ΔG_{OW} difference of only -1.2 kcal/mol at 25 °C. Interestingly, the enthalpic contribution ΔH_{OW} is positive (+4.1 kcal/mol), while the entropic contribution is negative (-5.3 kcal/mol), indicating that the partitioning of 18C6 to the chloroform phase is governed by entropy, as for hydrophobic species. From our simulations, the best trend regarding the partitioning of 18C6 is observed with its “weakly polar” model only, used here in conjunction with the TIP3P water and OPLS chloroform models, suggesting that the most polar model is also too “hydrophilic”. In fact, increasing the q_O charges from -0.4 to -0.6 increases significantly the interaction energy of 18C6 with water ($\Delta\Delta E_{18\text{C}6/\text{water}} = -31 \pm 3$ kcal/mol), but not with chloroform ($\Delta\Delta E_{18\text{C}6/\text{chloroform}} = 0 \pm 2$ kcal/mol). Also note that the conformational properties of 18C6 are model- and environment-dependent (see snapshots in Supporting Information, Figures S11 and S12). For instance, when the q_O charges increase, some OC–CO dihedrals turn from *gauche* to *trans*, and 18C6 adopts different conformations in chloroform compared to water, as a compromise between intrasolute and solute/solvent interaction energies. Accurate calculation of free energies of transfer of 18C6 thus requires to precisely account for solvent dependent conformational properties as well as of

changes in solute/solvent and solvent/solvent interactions, including entropic components.

Arguably, simulations with fixed charge representations of the solvent and solutes exaggerate the polarity of the interfacial water molecules and the hydrophilic/hydrophobic balance of amphiphilic solutes. We thus decided to investigate the effect of explicit representation of polarization effects, that improves the description of water and ions at water surfaces.^{82,83} The results obtained with the POL model and q_O charges of -0.4 are shown in Figure 11. They confirm the surface activity of 18C6 ($\Delta A_{\text{IW}} = 4.8$, $\Delta A_{\text{IO}} = 5.2$ kcal/mol), but erroneously predict a partitioning to water, by a quite small amount, though ($\Delta A_{\text{OW}} \approx -0.4$ kcal/mol).

Transfer of the 18C6/ $t\text{BuNH}_3^+$ Pic^- Complex. Like for the free salt, several PMFs were calculated for the complexed cation, comparing different reaction coordinates, different constraints, either -0.4 or -0.6 q_O charges for 18C6, and testing the POL model. The different $\Delta A(d)$ curves are shown in Figure 12, while snapshots at the I, O, and W positions are shown in Supporting Information, Figures S14 to S17. Our first attempts started with the 18C6(-0.6) model, pulling either the CM(18C6/ $t\text{BuNH}_3^+$) from the interface to the bulk phases and letting the Pic^- anion free of constraints (PMF1), or pulling the CM(18C6/ $t\text{BuNH}_3^+$ Pic^-) (PMF2). The resulting $\Delta A(d)$ curves (Figure 12) display a minimum near the oil side of the interface where the complex and the Pic^- counterion are loosely paired. At the interface, the complex adopts different orientations, where the ring of 18C6 is either parallel or

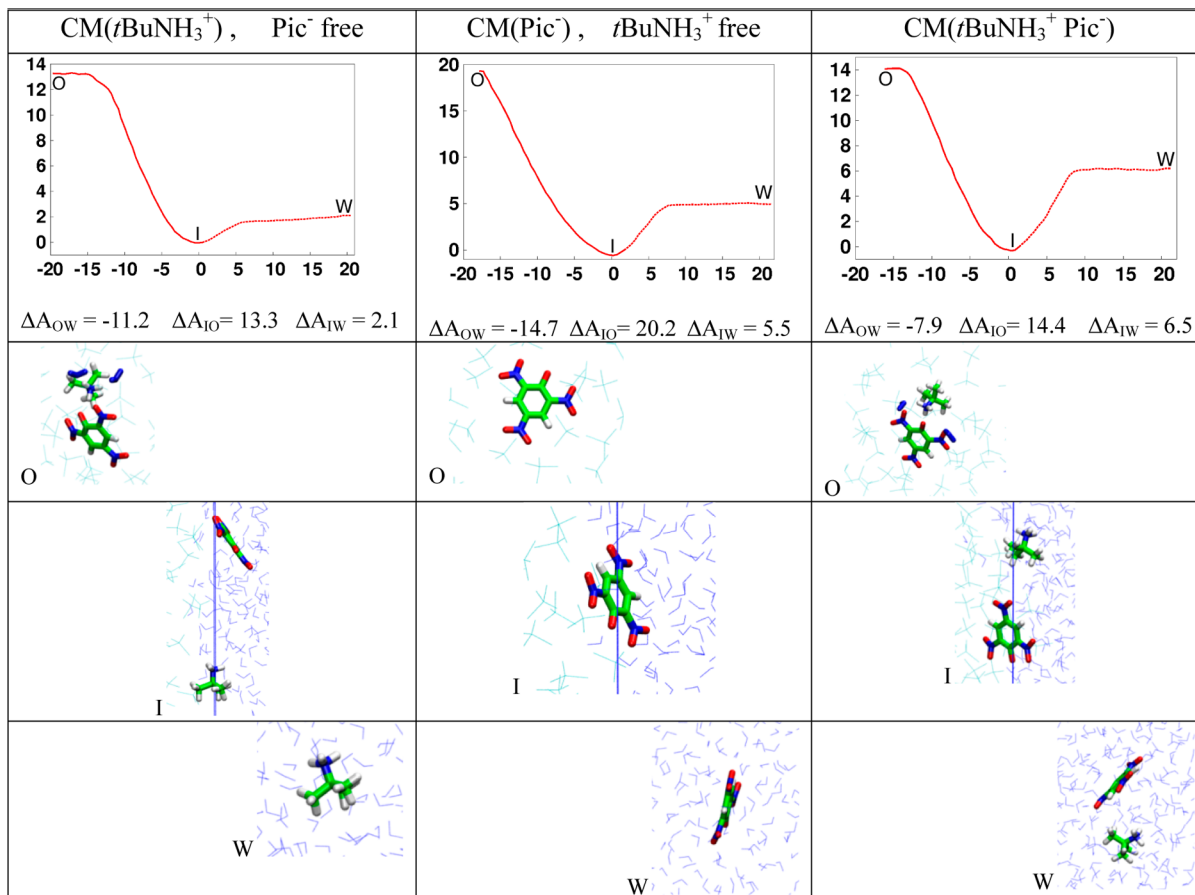


Figure 10. Transfer of $t\text{BuNH}_3^+ \text{Pic}^-$ across the chloroform/water interface: $\text{PMF}_{0.5+1}$ (ΔA in kcal/mol) calculated with three different reaction coordinates, and snapshots at O, I, and W positions.

perpendicular to the interface and the $t\text{Bu}$ group turns either toward water or in the plane of the interface. The transfer to the oil phase is energetically similar in PMF1 and PMF2 ($\Delta A_{IO} \approx +12$ kcal/mol), but corresponds to different states of the counterion: in PMF2, Pic^- follows the complex to the oil phase, while in PMF1 it stays at the interface. On the water side of the interface, PMF1 and PMF2 also somewhat differ: in both cases the complex dissociates while $t\text{BuNH}_3^+$ and Pic^- ions remain at the interface instead of moving to water, but 18C6 finally sits either in “bulk” water (PMF1) or at the other interface (PMF2; I_b position indicated in Figure 12). These features are consistent with the high surface activity of the salt and of 18C6 reported above, and with the low stability of the complex in water. In PMF1 and PMF2, the ΔA_{IW} energy difference is positive (≈ 6 and 3 kcal/mol, respectively), as for 18C6 itself. Neither PMF1 nor PMF2 predict, however, cation extraction by 18C6 to the oil phase, which is unexpected if one refers to the experimentally observed extraction of $t\text{BuNH}_3^+$ by 18C6 to chloroform.³¹

These results led us to consider a “preformed complex”, constrained to form a single entity where $t\text{BuNH}_3^+$ and Pic^- sit on opposite faces of the crown by imposing N(cation)...N(anion) distances of 5 to 6 Å, with harmonic constraints of 20 kcal/(mol·Å²). We compared the -0.4 to -0.6 q_O charge sets on 18C6 (PMF3 and PMF4, respectively). The resulting $\Delta A(d)$ curves (Figure 12) are similar and display a deep minimum at the interface, and still predict that the complex prefers the aqueous over the oil phase, by $\Delta A_{OW} = -2.3$ or

-4.2 kcal/mol, respectively. See Supporting Information, Table S8 for an energy component analysis.

We thus decided to test the influence of the electrostatic representation of the solute and of the solvents on the partitioning of the complex, and considered two variants (PMF5 and PMF6, respectively). In PMF5, the solute is described by ESP charges obtained by a QM/HF calculation on the whole 18C6/ $t\text{BuNH}_3^+\text{Pic}^-$ complex in the gas phase, yielding reduced charges on the $t\text{BuNH}_3^+$, Pic^- , and 18C6 moieties (0.71, -0.87, and 0.16 e, respectively). Note that these are close to those obtained in PCM–water (0.71, -0.91, and 0.20 e, respectively), indicating that the charges are little influenced by the surrounding solvent. The resulting $\Delta A(d)$ curve (Figure 12) is similar to the ones obtained in PMF3 or PMF4 with integer charges, still predicting a clear partitioning in water ($\Delta A_{OW} = -6.9$ kcal/mol). The second variant (PMF6) uses the POL model, in conjunction with integer charges on ions and $q_O = -0.6$ e on 18C6. Because of computer time limitations, PMF6 was conducted with a shorter sampling (0.1 + 0.5 ns per step) that we have checked to give for the transfer of 18C6 and of its constrained complex similar results as those obtained with 0.5 + 1.0 ns per step (see $\Delta A(d)$ curves in Figure 11 for 18C6 and Figure 12 for the complex). In fact, PMF6 confirms the deep minimum at the interface ($A_{IW} = 7.0$ and $A_{IO} = 8.1$ kcal/mol), but the A_{OW} energy (-1.1 kcal/mol) remains in favor of water over chloroform, by a smaller amount, however, than without polarization.

Taken together, these results suggest that, like for 18C6, the partitioning of the complex between the two phases involves a

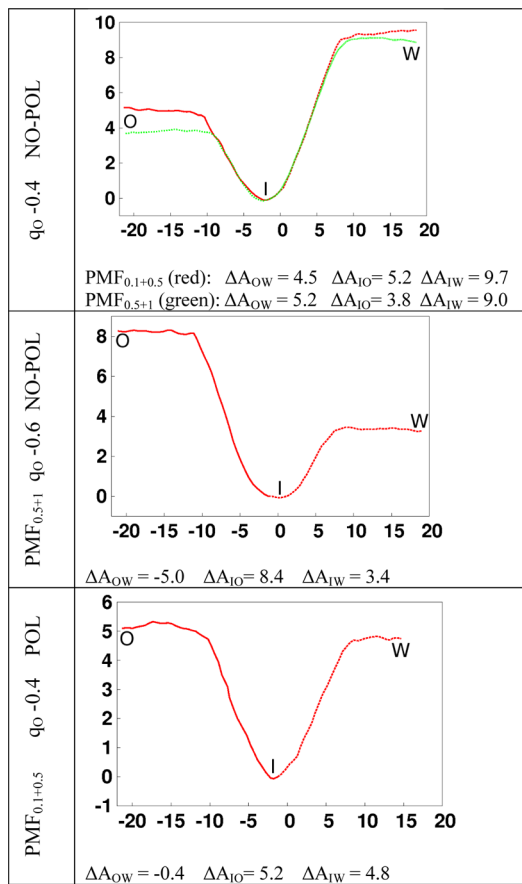


Figure 11. Transfer of 18C6 across the chloroform/water interface, simulated with different models: free energies (ΔA in kcal/mol) as a function of the distance of CM(18C6) to the interface (in Å). Snapshots at the O, I, and W positions are given in Supporting Information, Figures S12 and S13.

small energy difference, in the order of the kcal/mol, between the two phases. Quantitatively accounting for such a difference certainly requires more accurate and consistent energy representation (including electronic reorganization and non-additivity effects) of all partners involved in the complexation and transfer processes.

In addition to force field limitations, two distinguishing features, compared to extraction experiments should be noticed. First, the choice of the X^- anion, that was experimentally varied ($X^- = \text{Pic}^-, \text{ClO}_4^-, \text{SCN}^-, \text{Cl}^-$) so that measurements could be made on a wide range of compounds, and then corrected to the “ SCN^- scale”, assuming that SCN^- and Pic^- have the same free energies of transfer.³ We note that in the ClO_4^- , SCN^- , Cl^- series for which free energies of hydration ΔG_{hyd} are available,⁷⁶ the $\Delta \Delta G_{\text{hyd}}$ differences (0.0, -14.2, and -31.8 kcal/mol, respectively) are quite high, pointing to the importance of the X^- dehydration energy on the thermodynamics of transfer of the 18C6/ RNH_3^+ X^- complex to the oil phase. Second, in the oil phase, X^- forms a tight ion pair with RNH_3^+ (see PMF results in previous section) and the corresponding stabilization should also be X^- dependent. The simulated Pic^- anion used here may be somewhat too hydrophilic, attracting the complex in water. Another distinguishing feature, compared to real extraction systems concerns the concentration of 18C6 and the salt (for instance, about 0.1 M in ref 31). Since these species and their

complex are surface active, they should accumulate at the interface, thereby modifying its properties and, possibly, the precise partitioning and extraction equilibria.

DISCUSSION AND CONCLUSIONS

We have reported MD and PMF studies on the complexation of primary ammonium cations RNH_3^+ by 18C6 in nonaqueous media, in water, and in the gas phase as a reference. This extends the simulation studies on M^+ alkali ions complexation and recognition by 18C6,^{32–37} a simple “supramolecular” prototype for molecular recognition processes occurring in more complex systems, for instance in biology. We describe the free and complexed states of the cation in mixed solvents and, as reference, in their pure components, also comparing PrNH_3^+ to K^+ complexes. On the methodological side, we wanted to assess the performance of “routine” MD and PMF approaches to predict the complexation and recognition properties of 18C6 (i) in the monophasic chloroform/methanol mixture and in its pure components, (ii) and the biphasic chloroform/water mixture where experiments have been carried out. As seen above, this is far from being straightforward, since quantitative results depend on the electrostatic representation of 18C6 and the solvents. Owing to the simplicity of the force field and lack of explicit account of electron redistribution as a function of the environment (solvents, counterions, co-ions), no single model can consistently accurately account, for instance, for the conformational properties of the host, the complexation energies of different cations in various solvents, and the partitioning of the complexed or free ions between the aqueous and “oil” phases. The MD and PMF results cannot thus pretend to be quantitative, but are, with suitable electrostatic models, in qualitative accord with available experimental thermodynamic data in methanol and in water. The comparison of K^+ and PrNH_3^+ complexation in these two solvents turns out to be quite challenging, since the selectivity for K^+ and the higher stability of both complexes in methanol are hardly accounted for by PMF simulations without polarization (NO-POL models). The POL results are in better agreement with experiment, yet not quantitative. Beyond the prediction of molecular recognition in solution, the simulations afford microscopic views of the ammonium salt free and complexed in heterogeneous solutions and at the aqueous interface, as discussed below.

The Chloroform/Methanol Mixture Is Microscopically Heterogeneous and Displays Dual “Amphiphilic-like” Solvation Properties. Our simulations on the neat 90:10 mixture, and on its solutions with salts, 18C6 or their complex, clearly show that, despite their miscibility at all ratios, chloroform and methanol form a microscopically heterogeneous mixture, due to some self-aggregation of MeOH molecules. The methanol aggregates are small, quite labile in terms of size and composition, either isolated or connected by methanol chains. For instance, in the neat mixture (see snapshots and RDFs in Supporting Information, Figure S18), the aggregates contain ca. 4–10 MeOH molecules and each MeOH has 1.7 MeOH neighbors, according to the O···O RDF that peaks at ca. 3.5 Å. Aggregation is consistent with thermodynamic features like positive deviations from Raoult’s law for alcohols mixtures with nonpolar solvents,⁸⁴ large excess entropy of mixtures,^{85,86} and with recent MD simulations.⁸⁷ Self-association of methanol molecules has been likewise evidenced in CCl_4 by diffusion measurements⁸⁴ and NMR techniques.⁸⁸ Other fully miscible more polar liquids like

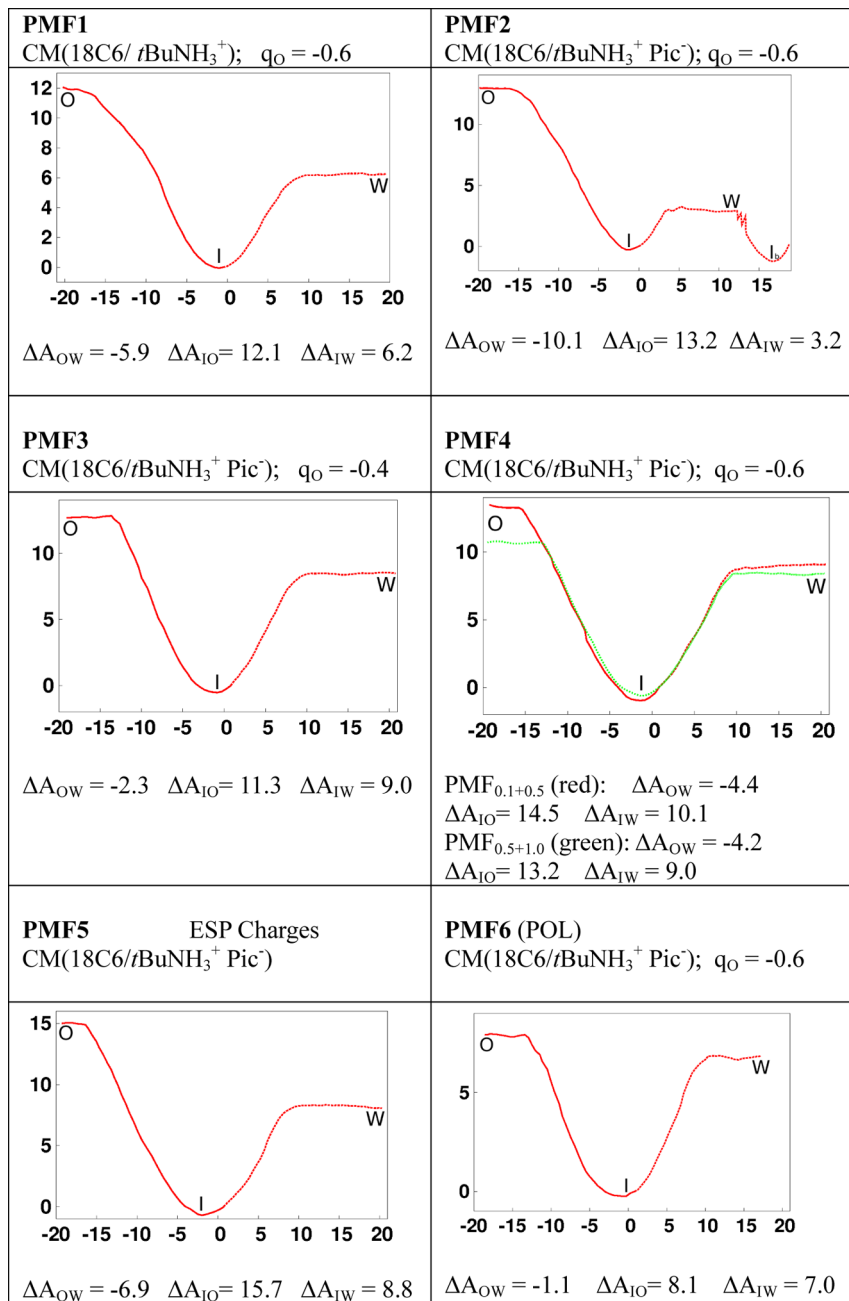


Figure 12. Transfer of the $18\text{C}6/t\text{BuNH}_3^+\text{Pic}^-$ complex across the chloroform/water interface with the complex either unconstrained (PMF1 and PMF2) or constrained (PMF3 to PMF6) and different electrostatic models. Full versions, including snapshots at the O, I, and W positions are given in Supporting Information, Figures S14 to S17.

water/methanol⁸⁹ or water/acetonitrile⁹⁰ form analogous, yet more dynamic, microscopically heterogeneous domains, thereby displaying dual solvation properties. As shown recently for THF/chloroform mixtures,⁹¹ interactions with the solute are mainly determined by the strongest couples, here $\text{RNH}_3^+ \dots \text{O}(\text{MeOH})$ and $\text{Pic}^- \dots \text{H}(\text{MeOH})$ hydrogen bonds for the salt and, to a lesser extent, $\text{O}(18\text{C}6) \dots \text{H}(\text{MeOH})$ interactions for the host. The CHCl_3 molecules afford weaker interactions and mostly solvate the less polar moieties of the solute, like $18\text{C}6$ or the alkyl group of the cation (see for instance snapshots in Figure 5 and Supporting Information, Figure S19). Since in the mixture, the methanol concentration is in excess over the solute, the thermodynamics of cation complexation is more “methanol-like” than “chloroform-like”. The $\text{RNH}_3^+ \text{Pic}^-$ ions,

strongly associated in chloroform, are loosely paired in the mixture, allowing for cation complexation without paying a high dissociation energy from its counterion. If one compares the free and complexed states of the cation in the mixture, the Pic^- counterion remains similarly solvated by the methanol molecules, and has thus little influence on complexation energies, as found here by simulations and experimentally²² in pure methanol solution. Noteworthy is the use of such mixtures for studying, for example, ammonium complexation by macrocyclic hosts combining aza-crown ether binding sites with lipophilic connectors that enjoy solvation by MeOH and CHCl_3 molecules, respectively.¹¹ The mixture also well solubilizes lipophilic and amphiphilic molecules and functions as membrane mimics for biological systems.⁹²

Ammonium Complexation and Extraction by 18C6: Importance of the “Oil”/Water Interface. According to the MD and PMF simulations, the $t\text{BuNH}_3^+$ Pic^- salt, 18C6 uncomplexed, and their complex are surface active and should thus accumulate at the oil/water interface. We are not aware of experimental data for the studied system, but evidence has been accumulated with analogues. For instance, 18C6 and its dibenzo- or dicyclohexyl-derivatives saturate the water/air interface at $\sim 10^{-1}$ M, 10^{-3} M, and 10^{-4} M concentrations, respectively.^{93,94} Kinetic and surface tension studies on the alkali cation transfer from water to “oil” phases pointed to the interfacial complexation reaction with the extractant molecule,^{95–98} also supported by interfacial electrochemistry studies.^{99–101} Alkylammoniums bearing long alkyl chains are cationic surfactants, forming monolayers at aqueous interfaces, with marked counterion effects.¹⁰² Generally speaking, the softer and more polarizable is the ion, the higher is its propensity to adsorb at the interface, following trends observed in the Hofmeister classification of ions.^{103–106} The fact that both RNH_3^+ and Pic^- ions and their complex are surface active is consistent with these views. Regarding the ion extraction process, the accumulation of reaction partners and the higher stability of the complex at the interface, compared to the aqueous phase, strongly hints for a complexation mechanism occurring mainly “at the interface”, i.e. in a nanosized thin domain of the solution. In agitated extraction systems, the interface “in action” can involve water microdroplets, as well as cylindrical or spherical micelles. Since about 15% of the 18C6 molecules partition in the aqueous phase, some complexation is also expected to occur there. To computationally visualize a “realistic” biphasic mixture, we simulated a water/chloroform solution containing 30 18C6 $t\text{BuNH}_3^+\text{Pic}^-$ species, including one 18C6/ $t\text{BuNH}_3^+$ complex, using the POL model and q_0 charges of -0.4 e on 18C6. The results after 5 ns of dynamics are shown in Figure 13. Remarkably, along the dynamics, five additional 18C6/ $t\text{BuNH}_3^+$ complexes formed spontaneously and adsorbed on the oil side of the interface. One of these formed in bulk water, while the four others formed at the interface (see the time evolution of their distances to the interface in Figure 13). The remaining uncomplexed 18C6 species are shared between the oil phase, the interface, and the bulk water, in keeping with the PMF results. Also note the formation of anionic Pic^- columns resulting from hydrophobic $\pi-\pi$ contacts between the picrate anions,¹⁰⁷ calling for further investigations on picrate salts at interfaces.

CONCLUSIONS

We report MD and PMF simulations on the complexation of protonated primary amines by 18C6 in solutions, focusing on the monophasic chloroform/methanol and the biphasic chloroform/water mixtures, and on their neat components, explicitly represented at the molecular level. Most results are in qualitative agreement with experiments, when available: the complexation free energies ΔG_{ass} in methanol and in water, the comparison of $t\text{BuNH}_3^+$ to PrNH_3^+ and K^+ guests, the partitioning of the $t\text{BuNH}_3^+\text{Pic}^-$ salt and of 18C6 uncomplexed in the oil/water mixture, with some dependence on the electrostatic model of 18C6, though. The results obtained in the chloroform/methanol mixture reveal the microscopic heterogeneity of the mixture that displays dual solvation properties toward the host, the ions, and their complex. The question of interface crossing upon assisted RNH_3^+ extraction is addressed, pointing to the surface activity

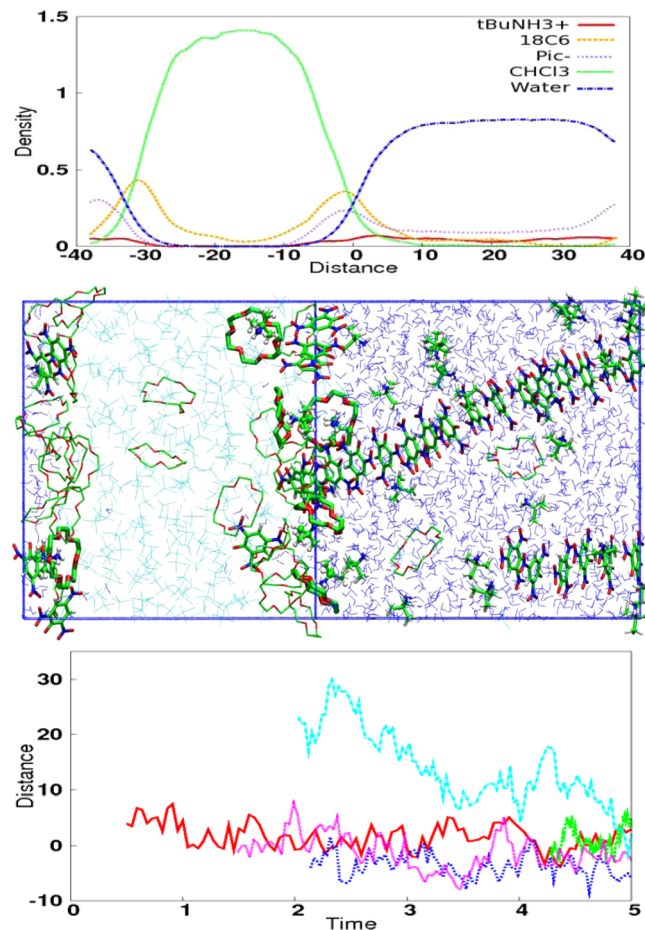


Figure 13. Thirty $[t\text{BuNH}_3^+ 18\text{C}6 \text{Pic}^-]$ at the chloroform/water interface ($q_0 = -0.4$ e; POL force field). From top to bottom: (i) density curves, (ii) snapshot after 5 ns of dynamics, and (iii) N(cation)...interface distance (in Å) of five complexes as a function of time (in ns), from the time of their formation along the dynamics.

of the crown ether, the salt alone, and their complex, hinting for an interfacial complexation and recognition mechanism. The results have bearing for other processes like ion separation by liquid–liquid extraction, or recognition and transport of biogenic amines through hydrophobic membranes.¹⁰⁸ There is certainly room for improving simulation methodologies regarding the energy representation (force field, QM/MM- or CPMD-type approaches) and the calculation of free energies of association in solution. Experimental structural and thermodynamics data (kinetics, surface tension, surface spectroscopies) on the studied solvent mixtures and interfaces should also contribute to improve our understanding of these complex heterogeneous solutions.

ASSOCIATED CONTENT

Supporting Information

Tables S1–S8 with atomic charges and polarizabilities, tests on QM versus AMBER interaction energies, energy components analysis, solvation features of the ammonium salts and their complex in different solvents. Figures S1 to S19 include snapshots of the simulated monophasic and biphasic systems, snapshots along the PMF trajectories and of chloroform/methanol mixtures. This material is available free of charge via the Internet at <http://pubs.acs.org>.

AUTHOR INFORMATION

Corresponding Author

*E-mail: wipff@unistra.fr.

Notes

The authors declare no competing financial interest.

ACKNOWLEDGMENTS

The authors are grateful to IDRIS, CINES, and Université de Strasbourg for computer resources, to Etienne Engler, Alain Chaumont, and Rachel Schurhammer for assistance and discussions, and for an ANR ILLA grant. This work is achieved within the LABEX “Chimie des systèmes complexes”.

REFERENCES

- (1) Späth, A.; König, B., Molecular Recognition of Organic Ammonium Ions in Solution Using Synthetic Receptors. *Beilstein J. Org. Chem.*, **2010**, *6* N° 32, doi:10.3762/bjoc.3766.3732.
- (2) Timko, J. M.; Helgeson, R. C.; Newcomb, M.; Gokel, G. W.; Cram, D. J. Structural Parameters That Control Association Constants between Polyether Host and Alkylammonium Guest Compounds. *J. Am. Chem. Soc.* **1974**, *96*, 7097–7099.
- (3) Cram, D. J.; Cram, J. M. Design of Complexes between Synthetic Hosts and Organic Guests. *Acc. Chem. Res.* **1978**, *11*, 9–14.
- (4) Cram, D. J. The Design of Molecular Hosts, Guests, and Their Complexes. *Angew. Chem. Int. Ed.* **1988**, *27*, 1009–1020.
- (5) Lehn, J. M. Design of Organic Complexing Agents. Strategies towards Properties. *Struct. Bonding (Berlin)* **1973**, *161*, 1–69.
- (6) Lehn, J. M. Cryptates: The Chemistry of Macropolycyclic Inclusion Complexes. *Acc. Chem. Res.* **1978**, *11*, 49–57.
- (7) Kotzyba-Hibert, F.; Lehn, J.-M.; Vierling, P. Multisite Molecular Receptors and Co-systems Ammonium Cryptates of Macrotricyclic Structures. *Tetrahedron Lett.* **1980**, *21*, 941–944.
- (8) Lehn, J. M. Cryptates: The Chemistry of Macropolycyclic Inclusion Complexes. *Acc. Chem. Res.* **1985**, *11*, 49–57.
- (9) Lehn, J. M. Supramolecular Chemistry—Scope and Perspectives. Molecules, Supermolecules and Molecular Devices (Nobel Lecture). *Angew. Chem., Int. Ed. Engl.* **1988**, *27*, 89–112.
- (10) Behr, J.-P.; Lehn, J.-M.; Vierling, P. Molecular Receptors. Structural Effects and Substrate Recognition in Binding of Organic and Biogenic Ammonium Ions by Chiral Polyfunctional Macrocylic Polyethers Bearing Amino-Acid and Other Side-Chains. *Helv. Chim. Acta* **1982**, *1853*–1867.
- (11) Kotzyba-Hibert, F.; Lehn, J. M.; Saigo, K. Synthesis and Ammonium Cryptates of Triply Bridged Cylindrical Macrotetracycles. *J. Am. Chem. Soc.* **1981**, *103*, 4266–4268.
- (12) Hamilton, A.; Lehn, J.-M.; Sessler, J. L. Coreceptor Molecules. Synthesis of Metalloreceptors Containing Porphyrin Subunits and Formation of Mixed Substrate Supermolecules by Binding of Organic Substrates and of Metal Ions. *J. Am. Chem. Soc.* **1986**, *108*, 5158–5167.
- (13) Trueblood, K. N.; Knobler, C. B.; Lawrence, D. S.; Stevens, R. V. Structures of the 1:1 Complexes of 18-Crown-6 with Hydrazinium Perchlorate, Hydroxylammonium Perchlorate, and Methylammonium Perchlorate. *J. Am. Chem. Soc.* **1982**, *104*, 1355–1362.
- (14) Gehin, D.; Kollman, P. A.; Wipff, G. Anchoring of Ammonium Cations to 18C6 Derivatives. *J. Am. Chem. Soc.* **1989**, *111*, 3011–3023.
- (15) Rüdiger, V.; Schneider, H. J.; Solov'ev, V. P.; Kazachenko, V.; Raevsky, O. A. Crown Ether-Ammonium Complexes: Binding Mechanisms and Solvent Effects. *Eur. J. Org. Chem.* **1999**, *1999*, 1847–1856.
- (16) Bühl, M.; Ludwig, R.; Schurhammer, R.; Wipff, G. Hydronium Ion Complex of 18-Crown-6: Theory Confirms Three “Normal” Linear Hydrogen Bonds. *J. Phys. Chem. A* **2004**, *108*, 11463–11468.
- (17) Olszewski, M.; Knop, S.; Seehusen, J.; Lindner, J.; Vöhringer, P. Ultrafast Internal Dynamics of Flexible Hydrogen-Bonded Supramolecular Complexes. *J. Phys. Chem. A* **2011**, *115*, 1210–1221.
- (18) Meot-Ner, M. Structurally Complex Organic Ions: Thermochemistry and Noncovalent Interactions. *Acc. Chem. Res.* **1984**, *186*–193.
- (19) Izatt, R. M.; Pawlak, K.; Bradshaw, J. S. Thermodynamic and Kinetic Data for Macrocycle Interaction with Cations, Anions, and Neutral Molecules. *Chem. Rev.* **1995**, *95*, 2529–2586.
- (20) Inoue, Y.; Gokel, G. *Cation Binding by Macrocycles. Complexation of Cationic Species by Crown Ethers*; M. Dekker, Inc.: New York and Basel, 1990.
- (21) Kauffmann, E.; Lehn, J. M.; Sauvage, J. P. Enthalpy and Entropy of Formation of Alkali and Alkali-Earth Macrobicyclic Cryptate Complexes. *Helv. Chim. Acta* **1976**, *59*, 1099–1111.
- (22) Izatt, R. M.; Lamb, J. D.; Izatt, N. E.; Rossiter, B. E., Jr; Christensen, J. J.; Haymore, B. L. , A Calorimetric Titration Study of the Reaction of Several Organic Ammonium Cations with 18-Crown-6 in Methanol. *J. Am. Chem. Soc.* **1979**, *101*, 6273–6276.
- (23) Bradshaw, J. S.; Baxter, S. L.; Scott, D. C.; Lamb, J. D.; Izatt, R. M.; Christensen, J. J. Complexation Properties of Macrocyclic Polyether-Diester Compounds Containing Furan and Benzene Subcyclic Units. *Tetrahedron Lett.* **1979**, *36*, 3383–3386.
- (24) Bradshaw, J. S.; Baxter, S. L.; Lamb, J. D.; Izatt, R. M.; Christensen, J. J. Cation-Complexing Properties of Synthetic Macrocyclic Polyether-Diester Ligands Containing the Furan, Benzene, Tetrahydrofuran, and Thiophene Subcyclic Units. *J. Am. Chem. Soc.* **1981**, *103*, 1821–1827.
- (25) Bradshaw, J. S.; Izatt, R. M. Crown Ethers: The Search for Selective Ion Ligating Agents. *Acc. Chem. Res.* **1997**, *30*, 338–345.
- (26) Habata, Y.; Bradshaw, J. S.; Young, J. J.; Castle, S. L.; Huszthy, P.; Pyo, T.; Lee, M. L.; Izatt, R. M. New Pyridino-18-Crown-6 Ligands Containing Two Methyl, Two *tert*-Butyl, or Two Allyl Substituents on Chiral Positions Next to the Pyridine Ring. *J. Org. Chem.* **1996**, *61*, 8391–8396.
- (27) Saigo, K.; Kihara, N.; Hashimoto, Y.; Lin, R.-J.; Fujimura, H.; Suzuki, Y.; Hasegawa, M. Synthesis and Selective Molecular Recognition of a Macrotricyclic Receptor Having Crown Ether and Cyclophane Subunits as Binding Sites. *J. Am. Chem. Soc.* **1990**, *112*, 1144–1150.
- (28) Zhu, C. Y.; Bradshaw, J. S.; Oscarson, J. L.; Izatt, R. M. Evaluation of a Direct ¹H NMR Method for Determining Log K and ΔH Values for Crown Ether-Alkylammonium Cation Complexation. *J. Incl. Phenom.* **1992**, *12*, 275–289.
- (29) Zhu, C. Y.; Izatt, R. M.; Bradshaw, J. S.; Dalley, N. K. A Thermodynamic and Structural Study of the Interactions of Pyridino- and Diketopyridino-18-Crown-6 Ligands with Some Primary Organic Ammonium Cations. *J. Incl. Phenom.* **1992**, *13*, 17–27.
- (30) Zhu, C.-Y.; Izatt, R. M.; Wang, T.-M.; Huszthy, P.; Bradshaw, J. S. Thermodynamic and Structural Studies of Cation-Macrocyclic Interaction. *Pure Appl. Chem.* **1993**, *65*, 1485–1492.
- (31) Timko, J. M.; Moore, S. S.; Walba, D. M.; Hiberty, P. C.; Cram, D. J. Host–Guest Complexation. 2. Structural Units That Control Association Constants between Polyethers and *tert*-Butylammonium Salts. *J. Am. Chem. Soc.* **1977**, *99*, 4207–4219.
- (32) Wipff, G.; Weiner, P.; Kollman, P. A. A Molecular Mechanics Study of 18-Crown-6 and Its Alkali Complexes: An Analysis of Structural Flexibility, Ligand Specificity, and the Macrocyclic Effect. *J. Am. Chem. Soc.* **1982**, *104*, 3249–3258.
- (33) Mazor, M. H.; McCommon, J. A.; Lybrand, T. P. Molecular Recognition in Nonaqueous Solvents. 2. Structural and Thermodynamic Analysis Selectivity of 18-Crown-6 in Methanol. *J. Am. Chem. Soc.* **1990**, *112*, 4411–4419.
- (34) van Eerden, J. V.; Harkema, S.; Feil, D. Molecular Dynamics of 18-Crown-6 Complexes with Alkali-Metal Cations: Calculation of the Relative Free Energies of Complexation. *J. Phys. Chem.* **1988**, *92*, 5076–5079.
- (35) Hay, B. P.; Rustad, J. R.; Hostetler, C. J. Quantitative Structure–Stability Relationship for K⁺ Ion Complexation by Crown Ethers. A Molecular Mechanics and *ab Initio* Study. *J. Am. Chem. Soc.* **1993**, *115*, 11158–11164.

- (36) Vayssi  re, P.; Chaumont, A.; Wipff, G. Cation Extraction by 18-Crown-6 to a Room-Temperature Ionic Liquid: The Effect of Solvent Humidity Investigated by Molecular Dynamics Simulations. *Phys. Chem. Chem. Phys.* **2004**, *7*, 124–135.
- (37) Chaumont, A.; Schurhammer, R.; Vayssi  re, P.; Wipff, G. Simulations of the Dynamics of 18-Crown-6 and Its Complexes: From the Gas Phase to Aqueous Interfaces with SC-CO₂ and with a Room-Temperature Ionic Liquid, In *Macrocyclic Chemistry: Current Trends and Future Perspectives*; Gloe, K., Ed.; Springer: Dordrecht, 2005; Chapter 21, pp 327–348.
- (38) Troxler, L.; Wipff, G. Interfacial Behaviour of Ionophoric Systems: Molecular Dynamics Studies on 18-Crown-6 and Its Complexes at the Water–Chloroform Interface. *Anal. Sci.* **1998**, *14*, 43–56.
- (39) Jost, P.; Galand, N.; Schurhammer, R.; Wipff, G. 222 Cryptand and Its Cryptates at the Water/Chloroform Interface: Molecular Dynamics Simulations of Concentrated Solutions. *Phys. Chem. Chem. Phys.* **2002**, *4*, 335–344.
- (40) Lauterbach, M.; Engler, E.; Muzet, N.; Troxler, L.; Wipff, G. Migration of Ionophores and Salts through a Water–Chloroform Liquid–Liquid Interface: Computer MD-PMF Investigations. *J. Phys. Chem. B* **1998**, *102*, 225–256.
- (41) Benay, G.; Wipff, G. Liquid–Liquid Extraction of Uranyl by TBP: The TBP and Ions Models and Related Interfacial Features Revisited by MD and PMF Simulations. *J. Phys. Chem. B* **2014**, *118*, 3133–3149.
- (42) Benay, G.; Wipff, G. Liquid–Liquid Extraction of Uranyl by an Amide Ligand: Interfacial Features Studied by MD and PMF Simulations. *J. Phys. Chem. B* **2013**, *117*, 7399–7415.
- (43) Guilbaud, P.; Wipff, G. MD Simulations on UO₂²⁺ and Sr²⁺ Complexes with CMPO Derivatives in Aqueous Solution and at a Water/Chloroform Interface. *New J. Chem.* **1996**, *20*, 631–642.
- (44) Benay, G.; Schurhammer, R.; Wipff, G. BTP-Based Ligands and Their Complexes with Eu³⁺ at “Oil”/Water Interfaces. A Molecular Dynamics Study. *Phys. Chem. Chem. Phys.* **2010**, *12*, 11089–11102.
- (45) Benay, G.; Wipff, G. Oil-Soluble and Water-Soluble BTPhens and Their Europium Complexes in Octanol/Water Solutions: Interface Crossing Studied by MD and PMF Simulations. *J. Phys. Chem. B* **2013**, *117*, 1110–1122.
- (46) Jayasinghe, M.; Beck, T. L. Molecular Dynamics Simulations of the Structure and Thermodynamics of Carrier-Assisted Uranyl Ion Extraction. *J. Phys. Chem. B* **2009**, *113*, 11662–11671.
- (47) Schweighofer, K.; Benjamin, I. Transfer of a Tetramethylammonium Ion across the Water–Nitrobenzene Interface: Potential of Mean Force and Nonequilibrium Dynamics. *J. Phys. Chem. A* **1999**, *103*, 10274–10279.
- (48) Benjamin, I. Recombination, Dissociation, and Transport of Ion Pairs across the Liquid/Liquid Interface. Implications for Phase Transfer Catalysis. *J. Phys. Chem. B* **2013**, *117*, 4325–4331.
- (49) Oberbrodhaege, J. Phase Transfer Catalysts between Polar and Non-polar Media: A Molecular Dynamics Simulation of Tetrabutylammonium Iodide at the Formamide/Hexane Interface. *Phys. Chem. Chem. Phys.* **2000**, *2*, 129–135.
- (50) Valente, M.; Sousa, S. F.; Magalh  es, A. L.; Freire, C. Transfer of the K⁺ Cation across a Water/Dichloromethane Interface: A Steered Molecular Dynamics Study with Implications in Cation Extraction. *J. Phys. Chem. B* **2012**, *116*, 1843–1849.
- (51) Case, D. A.; Darden, T. A.; Cheatham, T. E., III; Simmerling, C. L.; Wang, J.; Duke, R. E.; Luo, R.; Crowley, M.; Walker, R. C.; Zhang, W. et al., AMBER10, University of California: San Francisco, CA, 2008.
- (52) Cornell, W. D.; Cieplak, P.; Bayly, C. I.; Gould, I. R.; Merz, K. M.; Ferguson, D. M.; Spellmeyer, D. C.; Fox, T.; Caldwell, J. W.; Kollman, P. A. A Second Generation FF for the Simulation of Proteins, Nucleic Acids, and Organic Molecules. *J. Am. Chem. Soc.* **1995**, *117*, 5179–5197.
- (53) Jorgensen, W. L.; Briggs, J. M.; Contreras, M. L. Relative Partition Coefficients for Organic Solutes from Fluid Simulations. *J. Phys. Chem.* **1990**, *94*, 1683–1686.
- (54) Chang, T.-M.; Dang, L. X.; Peterson, K. A. Computer Simulation of Chloroform with a Polarizable Potential Model. *J. Phys. Chem. B* **1997**, *101*, 3413–3419.
- (55) Jorgensen, W. L.; Chandrasekhar, J.; Madura, J. D.; Impey, R. W.; Klein, M. L. Comparison of Simple Potential Functions for Simulating Liquid Water. *J. Chem. Phys.* **1983**, *79*, 926–936.
- (56) Frisch, M. J.; Trucks, G. W.; Schlegel, H. B.; Scuseria, G. E.; Robb, M. A.; Cheeseman, J. R.; Scalmani, G.; Barone, V.; Mennucci, B.; Petersson, G. A. et al., Gaussian 09 Revision B.01, Gaussian, Inc., Wallingford CT, 2010.
- (57) Dang, L. X.; Kollman, P. A. Free Energy of Association of the 18-Crown-6:K⁺ Complex in Water: A Molecular Dynamics Simulation. *J. Am. Chem. Soc.* **1990**, *112*, 5716–5720.
- (58) Dang, L. X.; Kollman, P. A. Free Energy of Association of the K⁺:18-Crown-6 Complex in Water: A New Molecular Dynamics Study. *J. Phys. Chem.* **1995**, *99*, 55–58.
- (59) Pohorille, A.; Jarzynski, C.; Chipot, C. Good Practices in Free-Energy Calculations. *J. Phys. Chem. B* **2010**, *114*, 10235–10253.
- (60) Kollman, P. A.; Caldwell, J. W. Structure and Properties of Neat Liquids Using Nonadditive Molecular Dynamics. Water, Methanol, and N-Methylacetamide. *J. Phys. Chem.* **1995**, *99*, 6208–6219.
- (61) Dang, L. X.; Chang, T. M. Many-Body Interactions in Liquid Methanol and Its Liquid/Vapor Interface: A Molecular Dynamics Study. *J. Chem. Phys.* **2003**, *119*, 9851–9857.
- (62) York, D. M.; Darden, T. A.; Pedersen, L. G. The Effect of Long-Range Electrostatic Interactions in Simulations of Macromolecular Crystals: A Comparison of the Ewald and Truncated List Methods. *J. Chem. Phys.* **1993**, *99*, 8345–8348.
- (63) Berendsen, H. J. C.; Postma, J. P. M.; van Gunsteren, W. F.; DiNola, A. Molecular Dynamics with Coupling to an External Bath. *J. Chem. Phys.* **1984**, *81*, 3684–3690.
- (64) Humphrey, W.; Dalke, A.; Schulten, K. VMD—Visual Molecular Dynamics. *J. Mol. Graphics* **1996**, *14*, 33–38.
- (65) Kollman, P. Free Energy Calculations: Applications to Chemical and Biochemical Phenomena. *Chem. Rev.* **1993**, *93*, 2395–2417.
- (66) Gumbart, J. C.; Roux, B.; Chipot, C. Efficient Determination of Protein–Protein Standard Binding Free Energies from First Principles. *J. Chem. Theory Comput.* **2013**, *9*, 3789–3798.
- (67) Cai, W.; Sun, T.; Liu, P.; Chipot, C.; Shao, X. Inclusion Mechanism of Steroid Drugs into β -Cyclodextrins. Insights from Free Energy Calculations. *J. Phys. Chem. B* **2009**, *113*, 7836–7843.
- (68) Roe, D. R.; Bergonzo, C.; Cheatham, T. E., III Evaluation of Enhanced Sampling Provided by Accelerated Molecular Dynamics with Hamiltonian Replica Exchange Methods. *J. Phys. Chem. B* **2014**, *118*, 3543–3552.
- (69) denOtter, W. K. Revisiting the Exact Relation between Potential of Mean Force and Free-Energy Profile. *J. Chem. Theory Comput.* **2013**, *9*, 3861–3865.
- (70) Gumbart, J. C.; Roux, B.; Chipot, C. Standard Binding Free Energies from Computer Simulations: What Is the Best Strategy? *J. Chem. Theory Comput.* **2013**, *9*, 794–802.
- (71) Deng, Y.; Roux, B. Computations of Standard Binding Free Energies with Molecular Dynamics Simulations. *J. Phys. Chem. B* **2009**, *113*, 2234–2246.
- (72) Prue, J. E. Ion Pairs and Complexes: Free Energies, Enthalpies, and Entropies. *J. Chem. Educ.* **1969**, *46*, 12–16.
- (73) Justice, M.-C.; Justice, J.-C. Ionic Interactions in Solutions. I. The Association Concepts and the McMillan-Mayer Theory. *J. Sol. Chem.* **1976**, *5*, 543–561.
- (74) Jorgensen, W. L. Interactions between Amides in Solution and the Thermodynamics of Weak Binding. *J. Am. Chem. Soc.* **1989**, *111*, 3770–3771.
- (75) Joung, I. S.; Cheatham, T. E., III Determination of Alkali and Halide Monovalent Ion Parameters for Use in Explicitly Solvated Biomolecular Simulations. *J. Phys. Chem. B* **2008**, *112*, 9020–9041.
- (76) Marcus, Y. *Ion Solvation*; Wiley: Chichester, UK, 1985.
- (77) Keesee, R. G.; Castleman, A. W. Thermodynamics of Gas-Phase Mixed-Solvent Cluster Ions: Water and Methanol on K⁺ and Cl[–] and Comparison to Liquid Solutions. *J. Phys. Chem.* **1991**, *95*, 3558–3564.

- (78) Koenig, K. E.; Lein, G. M.; Stuckler, P.; Kaneda, T.; Cram, D. J. Host-Guest Complexation. 16. Synthesis and Cation Binding Characteristics of Macrocyclic Polyethers Containing Convergent Methoxyaryl Groups. *J. Am. Chem. Soc.* **1979**, *101*, 3553–3566.
- (79) Ranghino, G.; Romano, S.; Lehn, J. M.; Wipff, G. Monte-Carlo Study of the Conformation-Dependent Hydration of the 18-Crown-6 Macrocycle. *J. Am. Chem. Soc.* **1985**, *107*, 7873–7877.
- (80) Paloncova, M.; Berka, K.; Otyepka, M. Convergence of Free Energy Profile of Coumarin in Lipid Bilayer. *J. Chem. Theory Comput.* **2012**, *8*, 1200–1211.
- (81) Takeda, Y.; Tanaka, A. Thermodynamic Study on Solvent Extraction of Alkali Metal Picrates with 18-Crown-6 into CHCl_3 . *Bull. Chem. Soc. Jpn.* **1986**, *99*, 733–736.
- (82) Jungwirth, P.; Tobias, D. J. Specific Ion Effects at the Air/Water Interface. *Chem. Rev.* **2006**, *106*, 1259–1281.
- (83) Wick, C. D.; Kuo, I. F. W.; Mundy, C. J.; Dang, L. X. The Effect of Polarizability for Understanding the Molecular Structure of Aqueous Interfaces. *J. Chem. Theory Comput.* **2007**, *3*, 2002–2010.
- (84) Prabhakar, S.; Weingärtner, H. The Influence of Molecular Association on Diffusion in the System Methanol–Carbon Tetrachloride at 25°C. *Z. Phys. Chem.* **1983**, *137*, 1278–1287.
- (85) Moelwyn-Hughes, E. A.; Missen, R. W. Thermodynamics Properties of Methyl Alcohol–Chloromethane Solutions. *J. Phys. Chem.* **1957**, *61*, 518–521.
- (86) Singh, P. P.; Sharma, B. R.; Sidhu, K. S. Thermodynamics of Chloroform and Methanol Mixtures. *Can. J. Chem.* **1979**, *57*, 387–393.
- (87) Gratias, R.; Kessler, H. Molecular Dynamics Study on Microheterogeneity and Preferential Solvation in Methanol/Chloroform Mixtures. *J. Phys. Chem. B* **1998**, *102*, 2027–2031.
- (88) Koch, W.; Leiter, H.; Mal, S. Z. A Study of Association in the System Methanol– CCl_4 by the Nuclear Magnetic-Relaxation Method. *Z. Phys. Chem. Neue Folge* **1983**, *136*, 89–99.
- (89) Pascal, T. A.; Goddard, W. A. III Hydrophobic Segregation, Phase Transitions and the Anomalous Thermodynamics of Water/Methanol Mixtures. *J. Phys. Chem. B* **2012**, *116*, 13905–13912.
- (90) Marcus, Y. The Structure of and Interactions in Binary Acetonitrile + Water Mixtures. *J. Phys. Org. Chem.* **2012**, *25*, 1072–1085.
- (91) Cook, J. L.; Hunter, C. A.; Low, C. M. R.; Perez-Velasco, A.; Vinter, J. G. Preferential Solvation and Hydrogen Bonding in Mixed Solvents. *Angew. Chem., Int. Ed.* **2008**, *47*, 6275–6277.
- (92) Pervushin, K. V.; Arseniev, A. S. Three-Dimensional Structure of (1–36)Bacteriorhodopsin in Methanol–Chloroform Mixture and SDS Micelles Determined by 2D ^1H -NMR Spectroscopy. *FEBS* **1992**, *308*, 190–196.
- (93) Vandegrift, G. F.; Delphin, W. H. Interfacial Activity of Liquid–Liquid Extraction Reagents -III: Crown Ethers. *J. Inorg. Nucl. Chem.* **1980**, *42*, 1359–1361.
- (94) Moyer, B. A., Complexation and Transport, In *Molecular Recognition: Receptors for Cationic Guests*; Atwood, J. L., Davies, J. E. D., McNicol, D. D., Vögtle, F., Lehn, J.-M., Eds.; Pergamon Elsevier: Oxford, UK, 1996; Vol. 1, Chapter 10, pp 377–416.
- (95) Danesi, P. R.; Chiarizia, R.; Pizzichini, M.; Saltelli, A. Transfer Rate of K^+ Ions from Aqueous Picrate Solutions into 1,2-Dichloroethane Solutions of the Macrocyclic Polyether Dibenzo-18-Crown-6. *J. Inorg. Nucl. Chem.* **1978**, *40*, 1119–1123.
- (96) Danesi, P. R.; Chiarizia, R.; Pizzichini, M.; Saltelli, A. Extraction Kinetics of 18C6 and DB18C6. *J. Inorg. Nucl. Chem.* **1978**, *40*, 1119–1123.
- (97) Yagodin, G. A.; Tarasov, V. V., Interfacial Phenomena in Solvent Extraction, In *Ion Exchange Solvent Extraction*; Marinsky, J. A., Marcus, Y., Eds.; Marcel Dekker: New York, 1984; Vol. 10, pp 141–237.
- (98) Szymanowski, J. Kinetics and Interfacial Phenomena. *Solv. Extract. Ion Exch.* **2000**, *18*, 729–751.
- (99) Senda, M.; Kakiuchi, T.; Osakai, T. Electrochemistry at the Interface between Two Immiscible Electrolyte Solutions. *Electrochim. Acta* **1991**, *36*, 253–262.
- (100) Beattie, P. D.; Delay, A.; Girault, H. H. Investigation of the Kinetics of Assisted K^+ Ion Transfer by DB-18C6 at the Micro-ITIES by Means of Steady-State Voltammetry. *J. Electroanal. Chem.* **1995**, *380*, 167–175.
- (101) Kazarinov, V. E. *The Interface Structure and Electrochemical Processes at the Boundary between Two Immiscible Liquids*; Springer Verlag: Berlin, 1987.
- (102) Popov, A. N., Counterions and Adsorption of Ion-Exchange Extractants at the Water/Oil Interface, In *The Interface Structure and Electrochemical Processes at the Boundary between Two Immiscible Liquids*; Kazarinov, V. E., Ed.; Springer Verlag: Berlin, 1987; pp 179–205.
- (103) Cacace, M. G.; Landau, E. M.; Ramsden, J. J. The Hofmeister Series: Salt and Solvent Effects on Interfacial Phenomena. *Q. Rev. Biophys.* **1997**, *30*, 241–277.
- (104) Collins, K. D.; Washabaugh, M. W. The Hofmeister Effect and the Behaviour of Water at Interfaces. *Quater. Rev. Biophys.* **1985**, *18*, 323–422.
- (105) Kunz, W.; Nostro, P. L.; Ninham, B. W. The Present State of Affairs with Hofmeister Effects. *Curr. Opin. Coll. Interface Sci.* **2004**, *9*, 1–18.
- (106) Vrbka, L.; Mucha, M.; Minofar, B.; Jungwirth, P.; Brown, E. C.; Tobias, D. J. Propensity of Soft Ions for the Air/Water Interface. *Curr. Opin. Colloid Interface Sci.* **2004**, *9*, 67–73.
- (107) Troxler, L.; Harrowfield, J. M.; Wipff, G. Do Picrate Anions “Attract Each Other” in Solution? Molecular Dynamics Simulations in Water and in Acetonitrile Solutions. *J. Phys. Chem. A* **1998**, *102*, 6821–6830.
- (108) Lehn, J. M., Chemistry of Transport Processes—Design of Synthetic Carrier Molecules. In *Physical Chemistry of Transmembrane Ion Motions*; Spach, G., Ed.; Elsevier: Amsterdam, 1983; Vol. 24, pp 181–206.